ABSTRACT

| | |
|---|---|
| Title of Document: | COPPER CORROSION IN THE FLOWERS OF SULFER TEST ENVIRONMENT. |
| | Dinesh Michael Mahadeo, M.S. Mechanical Engineering, 2015 |
| Directed By: | Professor Michael Pecht<br>Chair Professor and Director of the Center for Advanced Life Cycle Engineering(CALCE)<br>Department of Mechanical Engineering |

Sulfur, present in the environment in the form of sulfur dioxide and hydrogen sulfide, can produce failure in electronics. In particular, copper, which is used extensively in electronic products, is subject to corrosion in the presence of sulfur. This thesis examines the corrosion of copper under the Flowers of Sulfur (FoS) test at varying temperatures and durations. The FoS test setup, described in ASTM B809, was initially designed to evaluate surface finish porosity, but this setup may have boarder application. To expand the applicability of the FoS test, it is important to characterize the test environment. To this end, a systematic study of copper corrosion was conducted through weight gain measurements of copper coupons that were subjected to FoS test environments. From the test results, a model was developed that correlates copper sulfide thickness to temperature and time under the FoS test. This model can be used to determine test conditions given a target field environment.

COPPER CORROSION IN THE FLOWERS OF SULFER TEST ENVIRONMENT


By


Dinesh Michael Mahadeo




Thesis submitted to the Faculty of the Graduate School of the
University of Maryland, College Park, in partial fulfillment
of the requirements for the degree of
Master of Science
2015




Advisory Committee:
Professor Michael Pecht, Chair
Dr. Michael Osterman
Professor Patrick McCluskey

# Dedication

I dedicate this to my grandparents, parents, and brother for their love and support.

# Acknowledgements

# Table of Contents

# List of Tables

# List of Figures

# Chapter 1: Introduction to Corrosion

## 1.1 Corrosion and Electronics

Corrosion can be defined as the "destructive attack of a metal by chemical reaction with its environment" [1]. In a corrosion process, the pure metal is "destroyed"; it no longer exists after it forms corrosion products. Mechanical methods of destruction, such as abrasion, are not considered corrosion, as corrosion is a chemical process. Corrosion is caused by the flow of electrons in metal [2]. This can occur from one region of a metal to another region of that same metal or from one metal to another metal. This flow occurs as the result of an electrolyte being present between two areas with a potential between them. In cases where the electrolyte is water, anodic dissolution is the governing corrosion process [3]. Metal dissolves as ions into the water film formed on the metal surface, and then reacts with dissolved contaminants to form corrosion products [4]. These corrosion products have different properties than the base metal, which can lead to reliability concerns. An example of corrosion on a copper coupon is seen in Figure 1.
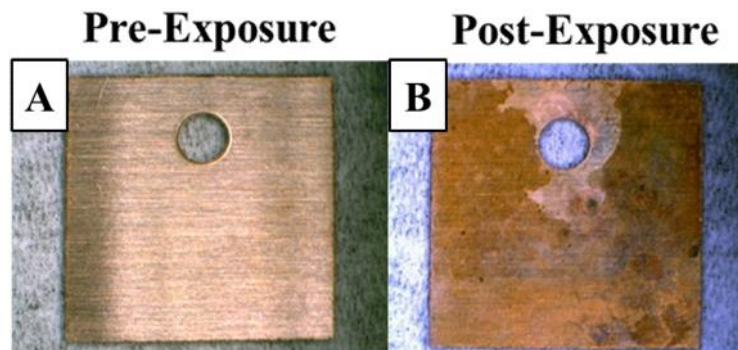


**Figure 1. Copper coupon before (A) and after (B) a corrosive**

Copper is commonly used in electronic systems due to superior mechanical,

electrical, and thermal properties [2]. It is soft and malleable, meaning that it is easily

machined. It also has excellent thermal and electrical conductivity. In electronics,

copper is used in applications where these superior electrical and thermal properties

are leveraged. It is used in printed circuit boards to create electrically conductive

paths between components mounted on the boards. Copper is also commonly used in

wires and connectors to create electrical connectivity. However, copper is susceptible

to atmospheric corrosion by sulfur-containing gases. Figure 2 provides an overview

of the formation of copper sulfide corrosion product.
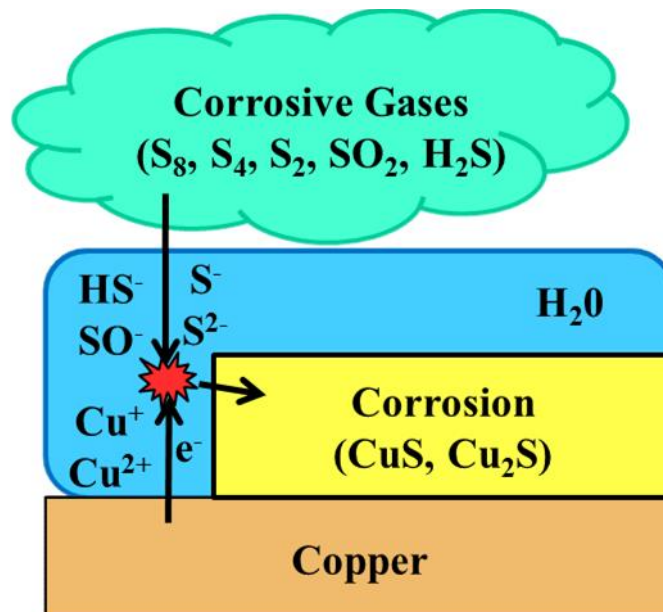


**Figure 2. Copper corrosion in a sulfur-containing atmosphere**

Atmospheric corrosion is a concern for copper-containing electronics in a variety of

environments [1]. Industrial, marine, tropical, and urban environments may contain

pollutants and moisture that can attack exposed metal on electronics. Power plants,

petroleum refineries, iron-smelting facilities, mines, pulp-processing facilities, and

sewage treatment plants all have corrosive environmental sulfur present in the field environment.

The corrosivity of any given environment can be affected by several different parameters in that environment [5]. The level of moisture found in an environment or the amount of humidity can have a significant effect on the rate of corrosion [6]. Contaminant level also has an effect on the rate of corrosion in different environments [7]. The presence of different contaminants can further complicate the rate of corrosion in a given environment [8]. Humidity, temperature, and contaminant level all contribute to the corrosivity of an environment.

*1.2 Laboratory Corrosion Testing for Electronics*

Laboratory corrosion testing for electronic products can serve several purposes. Corrosion tests can be carried out as part of failure analysis to replicate failures in order to identify failure sites and understand failure mechanisms. Corrosion tests can be carried out to analyze a group of parts, either to screen out bad parts or to compare different designs. These different uses for corrosion testing of electronics are summarized in Figure 3.
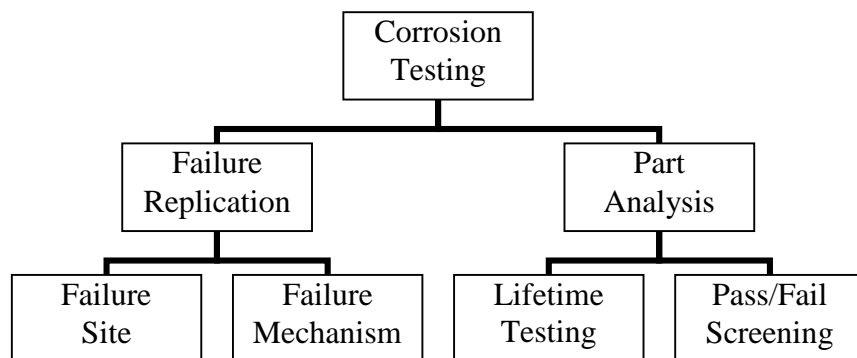


**Figure 3. Applications for Laboratory Corrosion Testing**

Electronic parts and systems fail in the field due to corrosion [10]. Corrosion testing of electronics is used to understand where, how, and why these failures occur. Devices that fail in the field can end up being damaged in multiple places, making failure analysis difficult. Laboratory testing allows for controlled exposure that is used to create failures in similar parts. Traditional failure analysis is carried out on laboratory-failed parts in order to identify weak points that can become failure sites [31]. Analyzing laboratory-failed parts is useful in understanding corrosion failure mechanisms .

Laboratory corrosion tests can also be used to examine parts during the research or manufacturing steps of the product design process [11]. Depending on the application, corrosion susceptibility can be a concern during the design of an electronic part or system. During prototyping, several designs can be compared using corrosion tests of varying severity. The severity of these tests can be correlated with different lifetime conditions in the field. Depending on how well the different designs are able to resist corrosion, they can be rated. Corrosion susceptibility then becomes one of the design factors that can be used when selecting which design to use. This applies not only to evaluating individual parts, but complete assemblies. If the application environment is more well established, laboratory corrosion testing can be used to screen parts [12]. Tests can be calibrated based on the purpose of the exposure in order to create a pass or fail system.

*1.3 Corrosion Test Methods*

Several laboratory test methods exist in order to perform corrosion testing. As discussed above, these different test methods can have different uses based on the goal of the test. The Mixed Flowing Gas (MFG), Flowers of Sulfur (FoS), and Clay Test are all methods that have been used in the literature to generate corrosive test environments. The following sections give a brief overview of these methods.

### 1.3.A. Mixed Flowing Gas Test Method

The Mixed Flowing Gas test method was developed to replicate corrosion mechanisms observed in the field [7,10]. The test involves placing samples into a fixed volume that has a heater to raise the air temperature and fans for circulation. A mixture of corrosive gases (Hydrogen Sulfide, Sulfur Dioxide, Nitrogen Dioxide, and Chlorine) is flown through the chamber in order to corrode the samples. A humid air supply is used to add moisture into the MFG test environment. Sensors can be used to monitor the chamber and adjust test parameters such as concentration, temperature, and humidity. A schematic of the MFG is seen in the Figure 4 below. Figure 5 shows samples placed into the MFG chamber used in the research carried out at CALCE.
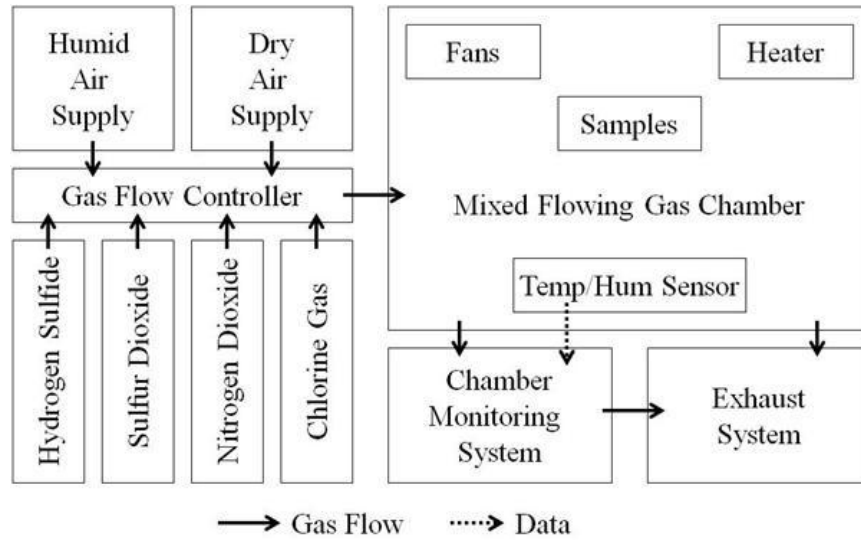
**Figure 4. Schematic of the MFG Test**
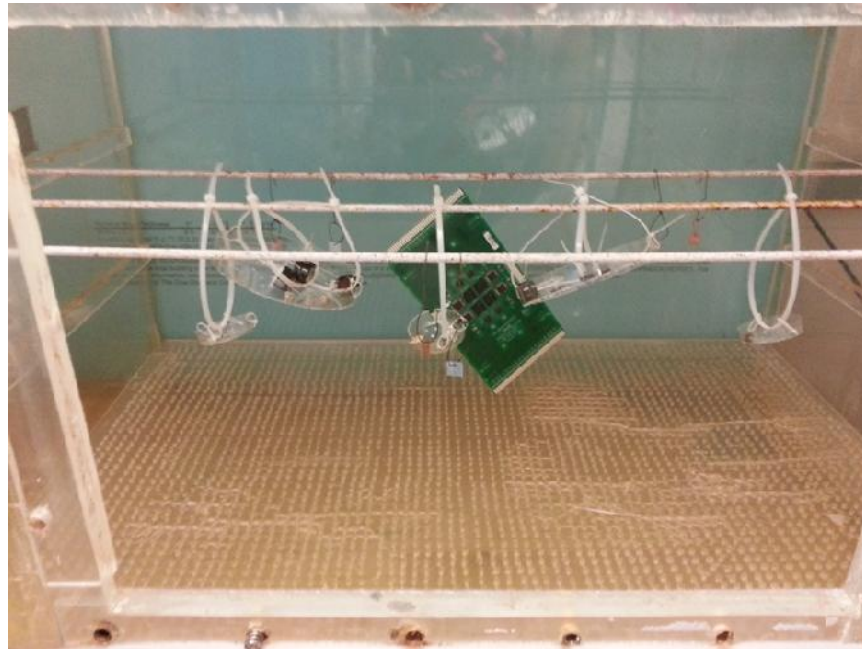


**Figure 5. Samples in the MFG chamber at CALCE**

The MFG test has been widely used in corrosion testing of electronics [3,5,6,10,15-21]. In most cases, the MFG is used as a lifetime test, where laboratory testing can be correlated to field conditions. In some cases, the MFG can be used as part of a pass/fail screening [31]. For these methods, the severity of the test must be fixed to a specific condition known to accelerate the failure mechanism that the test is meant to

be addressing. To achieve the goal of the MFG being a flexible test, several standards have been created that can be used to correlated the severity of the test to different field conditions.

Several different standards for running the MFG have been created, as seen in Table 1. The earliest MFG test conditions were created by William Abbott of Battelle Labs. In the Battelle test conditions, 2 days in chamber is supposed to correlate to 1 year in field [13]. The Battelle Environmental classification goes from least (Class I) to most(Class IV) corrosive environment. As Class I is a mild test condition, no MFG accelerated lab setup is given for that environment.

Electronic Industries Association (EIA) published their own set of MFG test conditions in EIA-364-65. This document used the three Battelle classes, but also provided modified versions for the class II and class III environments that included the addition of Sulfur Dioxide to catalyze the corrosion process. The addition of the sulfur dioxide changes the time correlation as 5 days in chamber is supposed to equal 3 years in field for the IIA and IIIA test conditions.

International Electro-technical Commission (IEC) also put out a set of standards to be used to test metallic coatings and electronic products. IEC Test Method 1 can be used as a corrosion test for gold plantings over reactive metals such as silver and copper. IEC Test Methods 2 and 4 are for electronic products in moderate corrosive environments, such as telecommunication centers and most office environments. IEC

Test Method 3 is appropriate for more severe corrosive environments, such as

electronic products deployed in industrial environments.


Telcordia and IBM both have developed corrosion test methods that are not correlated

with specific accelerations, but are meant to be representative of application

environments with varying severity. The Telcordia method has test conditions for

indoor and outdoor telecommunication applications. IBM's G1 test condition is

designed to replicate a generic business environment.

### Table 1. Test Conditions for the MFG

| Creator | Class | Temp (ºC) | RH (%) | H2S (ppb) | Cl2 (ppb) | NO2 (ppb) | SO2 (ppb) |
|---------|-------|-----------|--------|-----------|-----------|-----------|-----------|
| Battelle | II | 30±2 | 70±2 | 10+0/-4 | 10+0/-2 | 200±25 | --- |
| | III | 30±2 | 75±2 | 100±10 | 20±5 | 200±25 | --- |
| | IV | 50±2 | 75±2 | 200±10 | 50±5 | 200±25 | --- |
| EIA-364-65 | II | 30±2 | 70±2 | 10±5 | 10±3 | 200±25 | --- |
| | IIA | 30±1 | 70±2 | 10±5 | 10±3 | 200±25 | 100±20 |
| | III | 30±2 | 75±2 | 100±20 | 20±5 | 200±25 | --- |
| | IIIA | 30±1 | 70±2 | 100±20 | 20±5 | 200±25 | 200±50 |
| | IV | 40±2 | 75±2 | 200±20 | 30±5 | 200±25 | --- |
| IEC 68-2-60 | 1 | 25±1 | 75±3 | 100±20 | --- | --- | 500±100 |
| | 2 | 30±1 | 75±3 | 10±5 | 10±5 | 200±50 | --- |
| | 3 | 30±1 | 75±3 | 100±20 | 20±5 | 200±50 | --- |
| | 4 | 25±1 | 75±3 | 10±5 | 10±5 | 200±50 | 200±20 |
| Telcordia GR-63-CORE 5.5 | Indoor | 30±1 | 70±2 | 10±1.5 | 10±1.5 | 200±30 | 100±15 |
| | Outdoor | 30±1 | 70±2 | 100±15 | 20±3 | 200±30 | 200±30 |
| IBM | G1 | 30±.5 | 70±2 | 40±5% | 3±15% | 610±5% | 350±5% |

    1.3.B. Flowers of Sulfur Test Method

The Flowers of Sulfur test(ASTM-B809) is a corrosion test method published by the

American Society for Testing and Materials (ASTM) to be used in pass/fail porosity

testing [22]. The test involves suspending test samples in a sealed glass chamber.

Elemental sulfur, the namesake Flowers of Sulfur, is placed inside the sealed chamber

underneath the samples. In addition to the sulfur source, a Potassium Nitrate salt

solution is placed in the chamber. This solution is a saturated salt solution in

deionized water. The entire chamber is placed into an oven which is heated to 50 °C.

As the oven heats up, the solid elemental sulfur releases sulfur vapor into the

chamber. As the salt solution is heated up, moisture is released into the chamber

volume. The salt solution is saturated, meaning that the chamber will reach a known

humidity for a fixed temperature. As described in the ASTM-B809 standard, the test

is run for a 24 hour period, after which the test samples are removed. A schematic of

the FoS test is seen in Figure 6 below, while Figure 7 shows an image of the setup.
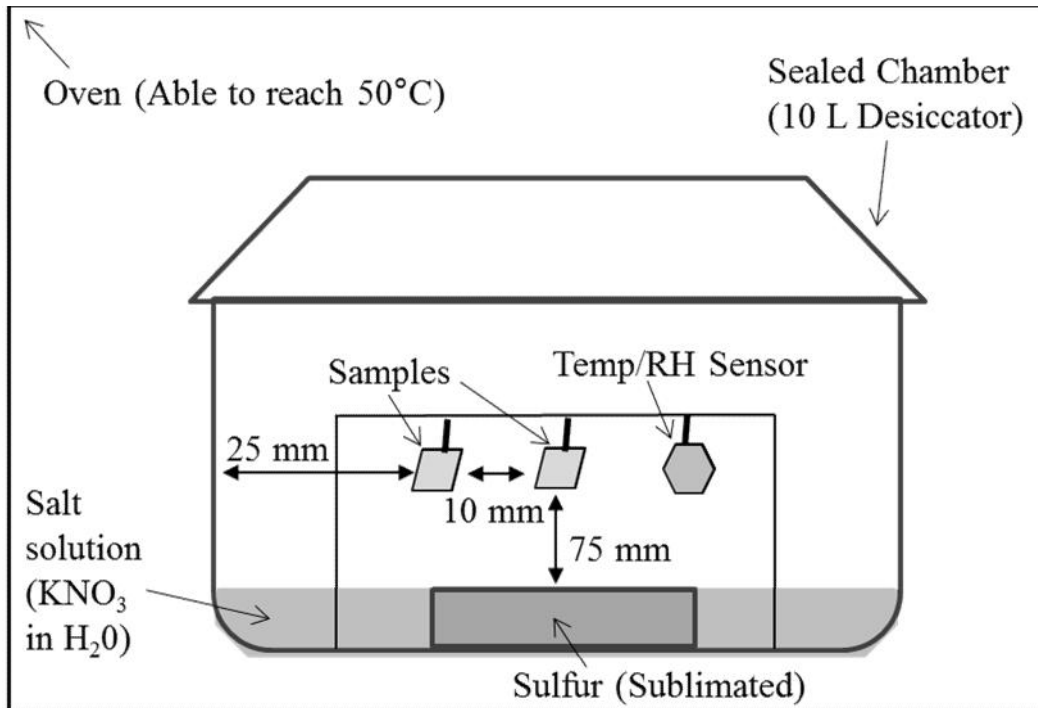


**Figure 6. Schematic of the Flowers of Sulfur Test**

9
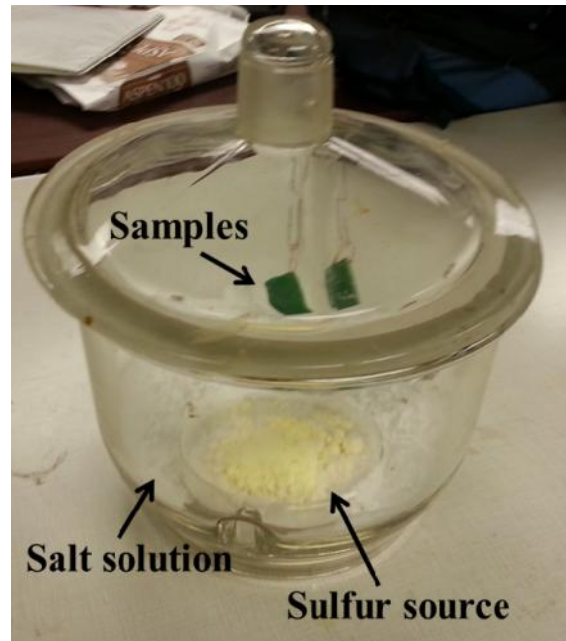
**Figure 7. Picture of the ASTM-B809 FOS Test setup**

<u>1.3.C. Clay Test Method</u>

Clay Testing is a corrosion test method that has been used to replicate field failures in

the laboratory [23]. The method involves placing samples in a sealed container

containing modeling clay. The modeling clay is moistened and heated in a microwave

before and periodically during the exposure. The warm, moist clay serves both as a

sulfur and humidity source. This setup can generate corrosion on printed circuit

boards [24]. There is not a standard for carrying out this test method and several

approaches have been documented in the literature [23,24]. A schematic of the clay

test is seen in Figure 8 and a picture of an actual test is seen in Figure 9 [24].
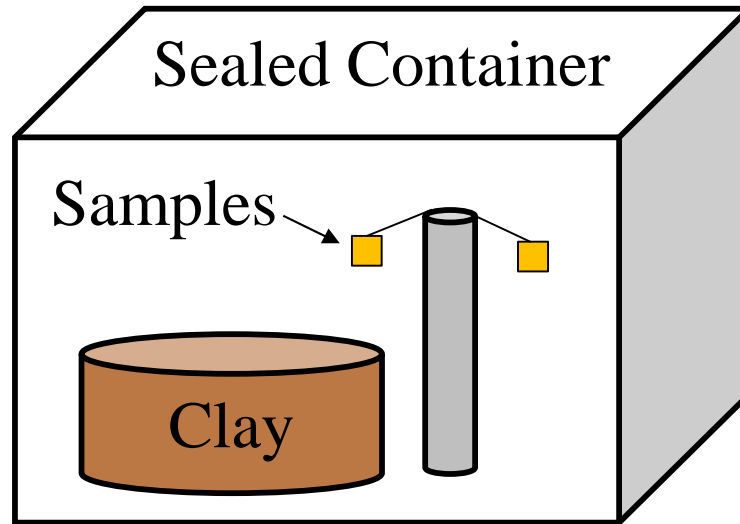
**Figure 8. Schematic for Clay Test**
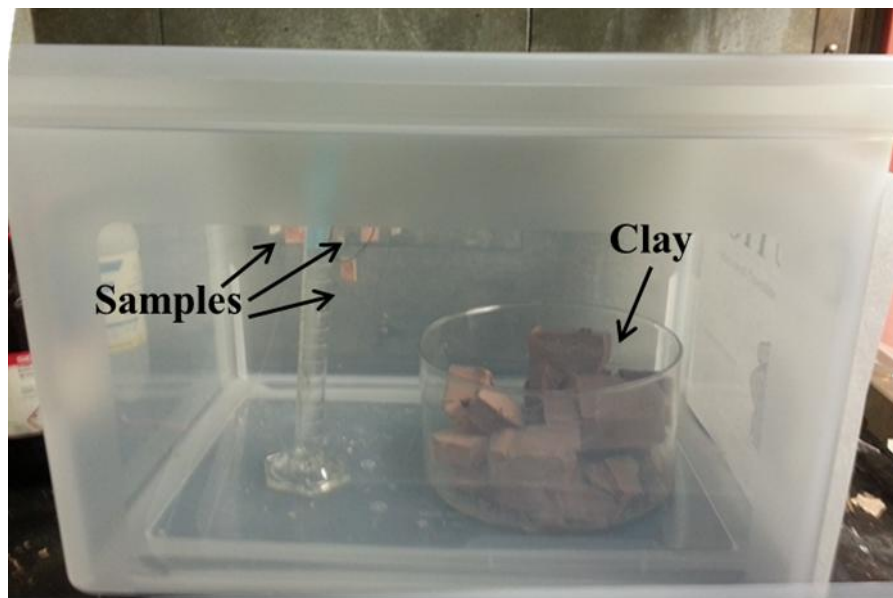


**Figure 9. Picture of a clay test carried out at CALCE**

1.3.D. Comparison of Corrosion Test Methods

As mentioned previously, each of these methods has advantages and disadvantages. A brief comparison of these corrosion test methods is in the table below. The MFG allows for multiple sulfur sources and the inclusion of chlorine. Temperature and gas concentration are independently controlled, and the fans in the chamber ensure that

11

air flows over the samples. However, the MFG is the most difficult of the three to
setup, as it requires specialized equipment and facilities, and requires periodic
monitoring while it ramps up and even when it is running. The FOS however is
simpler to setup and has the advantage of having pure elemental sulfur as the sulfur
source. Since the FOS is carried out in an oven, the temperature of the FOS can be
much higher than the other two test methods. Additional advantages to the FOS that
make it appealing as a corrosion test include a simple setup, and few consumables.
However, in the FOS there are no oxidation accelerants such as Nitrogen Dioxide.
There is also an inverse relationship between temperature and humidity that can end
up being a problem at very high temperatures (>90°C). The clay test method is the
easiest to setup, as it does not require a special chamber or even an oven. Clay is a
realistic sulfur source that can provide both moisture and sulfur. However the clay
test setup needs constant reheating and can only be carried out at a low temperature.

**Table 2. Comparison of Methods**

| Method | Advantages | Disadvantages |
|--------|-----------|---------------|
| MFG | - Multiple sulfur sources<br>- Independent conc./temperature<br>- Can have chlorine<br>- Forced convection | - Difficult to setup<br>- Requires monitoring |
| FOS | - High maximum temperature<br>- Pure elemental sulfur | - No oxidation accelerants<br>- Inverse Temperature/Humidity |
| Clay | - Simple setup<br>- Realistic sulfur source | - Constant reheating<br>- Low temperature |

Corrosion of copper coupons in test environments is used to assess the severity of the environment, either by comparison to environmental standards or field data [9]. Research has been done on classification of corrosive environments [10] and standards exist for the use of copper coupons as witness samples for corrosive test environments [14]. The relationship between copper film thickness and various environmental factors is well documented in the literature [6].

Different classification schemes exist, based on different classification schemes. The Battelle classification is based on correlating MFG exposures to corrosion levels in the field [13]. The development of this method used cathodic reduction to determine film thickness. Table 3 shows the Batelle classification for corrosive environments based on corrosion film thickness of copper.

**Table 3. Battelle corrosion classes for environment severity**

| Battelle | |
|---|---|
| Severity Class | 1 year film thickness |
| I | <35 nm |
| II | 40 to 70 nm |
| III | 80 to 400 nm |
| IV | >500 nm |

The International Society for Automation (ISA) created ISA Standard 71.04-1985 for

classification of corrosive environments when carrying out corrosion monitoring [25].

These classifications allows users to determine the corrosive potential of a particular

environment towards electronic equipment. The standard describes two different

methods of environmental characterization: concentration monitoring and reactivity

monitoring. Concentration monitoring is carried out by measuring the contaminants

in an environment, while reactivity monitoring is carried out by measuring the

thickness of the corrosion film formed on a sample of exposed copper using weight

gain measurements. The classes described in the ISA standard have also been adopted

by the American Society of Heating, Refrigerating and Air-Conditioning Engineers in

their guidelines for suitable data center environments [26]. The classes outlined in the

ISA standard are presented in Table 4.

**Table 4. International Society for Automation (ISA) corrosion classes**

| International Society for Automation (ISA) | |
|---|---|
| Severity Level | 30 Day film thickness |
| G1 – Mild | <30 nm |
| G2 – Moderate | 30 to 100 nm |
| G3 - Harsh | 100 to 200 nm |
| GX - Severe | >200 nm |

Several methods exist for quantifying the thickness of the copper corrosion film. Weight gain techniques rely on using a measurement of the weight change of corroded samples to calculate the expected film thickness based on a known relationship between weight gain and film thickness. In some methods, and in this thesis, copper coupons are weighed before and after exposure and the change in weight is used to calculate the corrosion film thickness. In other methods, quartz crystal microbalances are used to measure the changing weight of a copper membrane in real time. The change in weight is converted to a thickness estimate using assumptions about composition and uniformity.

The major drawback of this method is that there are assumptions about the corrosion film that go into the calculations that are known to be flawed. There is an assumption in calculating the corrosion film thickness from weight gain that the corrosion product is uniform over the entire exposed surface. As surface corrosion tends to occur more frequently at imperfection in the metal surface, this is almost never the case. There is also another assumption that the corrosion product is uniform for the entirety of the corrosion film. Corrosion is a surface phenomenon and the composition of the corrosion film can vary with depth.

Weight gain alone can be used as a corrosion metric. The major limitation is that the samples must be a fixed geometry and that the preparation of different samples should be easily reproducible. Reporting weight gain for fixed samples is more direct than using the weight gain and a series of assumptions to calculate an estimated

15

equivalent thickness. Another drawback that would need to be considered is that weight gain alone requires a pre-exposure and post-exposure measurement. If corrosion film thickness is used to classify an environment, one of the other methods described later on can be used to calculate the thickness, but this is not the case with a weight gain-based classification system. Nonetheless, as corrosion film thickness is used in the literature to classify corrosive environments conversion from weight gain to film thickness are made in this paper.

Another commonly used method for corrosion thickness measurement is cathodic reduction. In this method, the reactions that form the corrosion process is reversed by applying a bias in an ionic solution. After the corrosion product has been reversed, the current drawn from the power source changes. The amount of charge used in this reversal can be used to estimate the thickness of the corrosion layer. This method has been demonstrated to underestimate corrosion film thickness. As the reduction is carried out, areas with a thinner film have copper exposed faster. This is what terminates the chemical reaction part of the process and thus may end up leaving areas with corrosion product still available.

A final method used to measure copper coupon corrosion thickness is profiliometry. In this technique an ion milling process is used to remove the corrosion film on a select area of a corroded sample until the bare metal is exposed. Optical or contact profiliometry can be used to measure the height of the corrosion film. While this is

the most direct method to measure corrosion film, the time and financial costs of

carrying out ion milling make it unpopular.

**Figure 10. Methods for measuring corrosion thickness**

Weight Gain
- Pro: Simple method
- Con: Bad assumption of products

Cathodic Reduction
- Pro: Does not require pre- exposure data
- Con: Underestimates corrosion

Profilometry
- Pro: Accurate measurement
- Cons: Requires ion milling
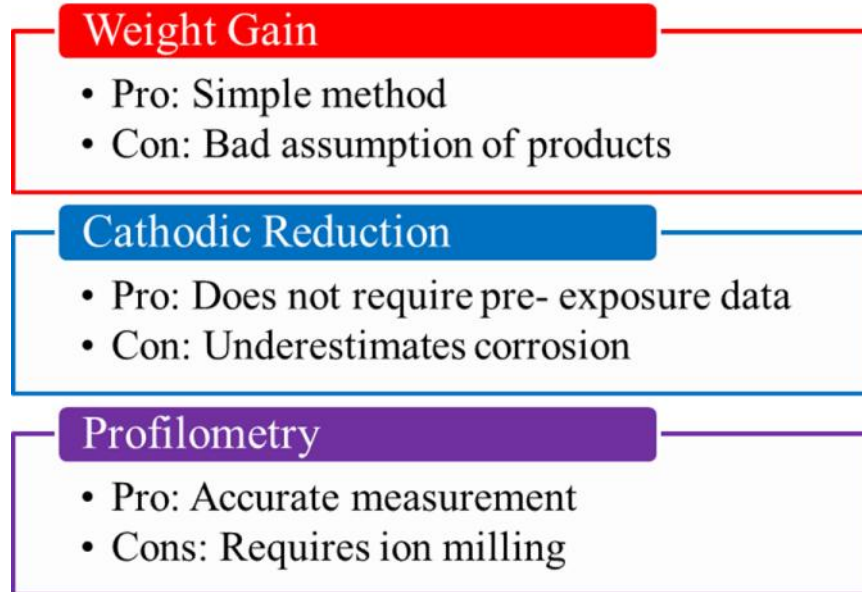
In this paper copper film thickness is calculated using the weight gain of copper

coupons placed into several different FOS environments. These measurements are

used to examine the relationship between test temperature, test duration, and film

thickness gain. A model is created for calculating expected copper film thickness,

which can be used in tandem with corrosion standards or field data to categorize the

severity of different FOS test environments.

# Chapter 2: Flowers of Sulfur Testing

## 2.1 Early History of Flowers of Sulfur (FOS) Testing

The Flowers of Sulfur Test method as described in this thesis refers specifically to the Flowers of Sulfur Test Method [ASTM B809] created by the American Society for Testing and Materials (ASTM) [22]. As stated in the standard, this test method was designed to evaluate the porosity of metallic coatings. This test is not designed to look at copper and silver films, but instead is used to evaluate how well films plated over those metals protect copper and silver (sec. 1.2).

This test environment is different than the Mixed Flowing gas test environment in that sulfur vapor is used as the corrosive sulfuric reactant (sec. 4.1). This is in contrast to the MFG test, where sulfur-containing gases such as $SO_2$ and $H_2S$ are used. The standard states that the test is used to simulate humid indoor atmospheric tarnishing, but acknowledges that the chemistry and the properties of corrosion films formed in the test environment may not resemble corrosion products from the field (sec 4.3/sec 5.3). The test is designed to be used on samples of different geometries, and is suitable for irregular surfaces (sec 5.7). However, ASTM makes it clear that the test is intended to evaluate porosity, and cannot be used to evaluate product performance or time to failure without additional information (sec 5.9).

## 2.2 Use of the FOS for Corrosion Testing of Electronics

In the literature, the use of the FOS test has been expanding. Early work using the test focused on porosity testing for surface finishes. This surface finish testing expanded into using the test for evaluating conformal coatings used to protect surface finishes [27, 28]. Flowers of Sulfur testing has gained considerable interest is the identification of susceptibility of silver-containing chip resistors to failure due to the formation of silver sulfide [29]. As seen in the figure below, chip resistors have an inner electrode layer that is made of silver. This silver layer is susceptible to corrosive attack in sulfur-containing environments. Either through cracking or separation of the protective layers, sulfur in the atmosphere can reach the inner electrode and corrode it away, causing resistor failure [30]. When the Mixed Flowing Gas (MFG) test failed to produce corrosion on chip resistors, researchers began searching for alternative accelerated corrosion tests that could prove suitable for replicating the failure mechanism. The FOS has been successful in replicating this failure mechanism in laboratory environments [31].
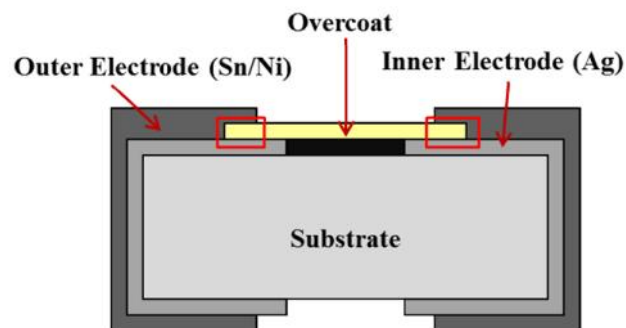


**Figure 11. Chip resistor (Failure sites highlighted)**

19

As of the writing of this thesis several different groups have taken an interest in

adaptations of the ASTM FOS test method. International Electronics Manufacturing

Initiative (iNEMI) has been carrying out FOS tests in a modified chamber as seen in

Figure 12 [32,33]. In this setup, the samples are mounted to printed circuit boards that

are attached to a motor in the test vessel. The motor spins the boards with the samples

above containers with the salt solution and elemental sulfur.
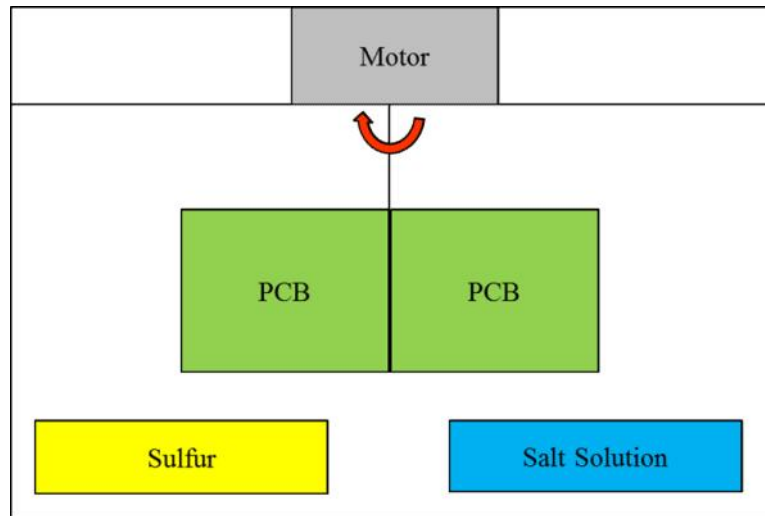


**Figure 12. iNEMI Modified Flowers of Sulfur Setup**

In the iNEMI test vessel, the speed of the motor was varied as well as the salt solution

in order to change the corrosivity of the test environment. As the mean air velocity

was increased from zero to 1.3 m/s, the copper corrosion rate rose from 2000 to

12000 Å/day [31]. In this test setup, tests were carried out with Potassium Chloride

instead of the Potassium Nitrate used in the ASTM FOS Standard. Copper corrosion

rates were observed to be higher in the Potassium Nitrate FOS setup(~2000 Å/day

compared to 800 Å/day copper corrosion rate). This corrosion test is being developed

as a screening method for printed circuit boards with surface finished that may have flux residue that acts as a contaminant. The IPC 3-11g committee is working on a screening method for chip resistors based on the ASTM FOS test setup. The absorption of sulfur by printed circuit boards placed into the FOS is being examined as a concern with the test.

*2.4 Corrosion Modeling for the Flowers of Sulfur Test*

Corrosion models usually represent the amount of corrosion, in this case the film thickness as a function of environmental factors and a time term [3,5,8]. The environmental factors can include a wide variety of different parameters, such as temperature, humidity, sulfur concentration, and the concentrations of any other oxidizing agents in the atmosphere [5]. This time term is usually a power function of time, with the power ranging from .5 to 1 [8]. For diffusion-limited reactions, the constant approaches .5 for longer time scales [3]. Equation 1 below shows corrosion film thickness ( ) [in nm] as a function of environmental factors ( ) and time (t).

$$= f(\ )*t^n \qquad [1]$$

Temperature, humidity, sulfur concentration and time are all environmental factors that affect the amount of corrosion that occurs in the FOS test environment. For these FOS tests, only temperature and time are independent parameters. Figure 13 shows the factors expected to influence copper corrosion and the relationship of humidity and sulfur to temperature.
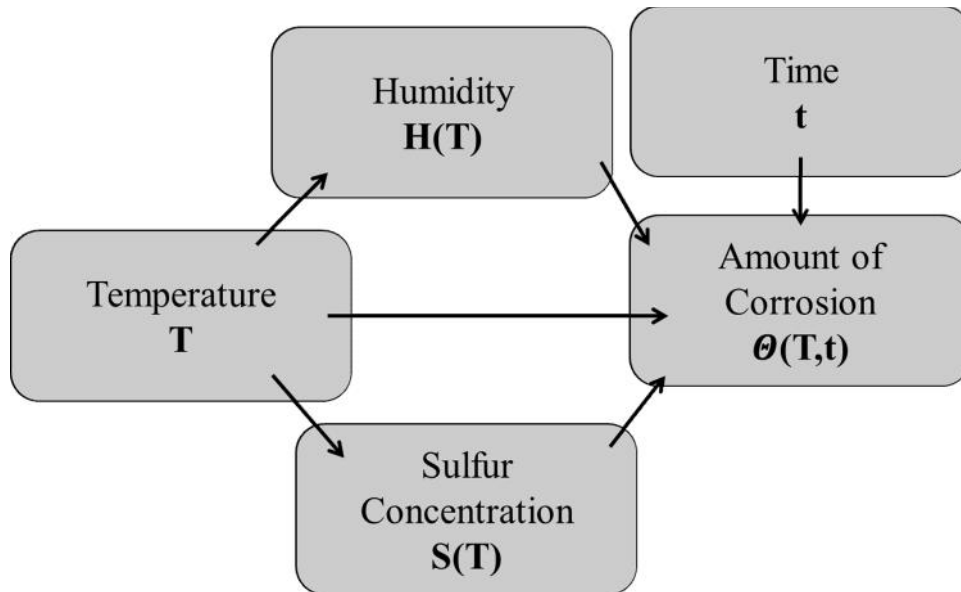
**Figure 13. Factors contributing to corrosion in the FOS**

If the only effect of increased temperature is driving the reaction of sulfur with the copper, the increase in corrosion product would follow an exponential relationship with temperature [16]. However, increasing the temperature of the FOS test vessel decreases the relative humidity in an atmosphere controlled by a saturated salt solution in a polynomial manner [17]. This was verified for the FOS vessel used in this thesis by measuring humidity in a FOS test without sulfur. The results can be seen in Figure 14. Figure 15 shows the data from this experiment plotted along with data from the literature [17]. A second order exponential fit that passes through the intercept at the value provided in the literature is shown.
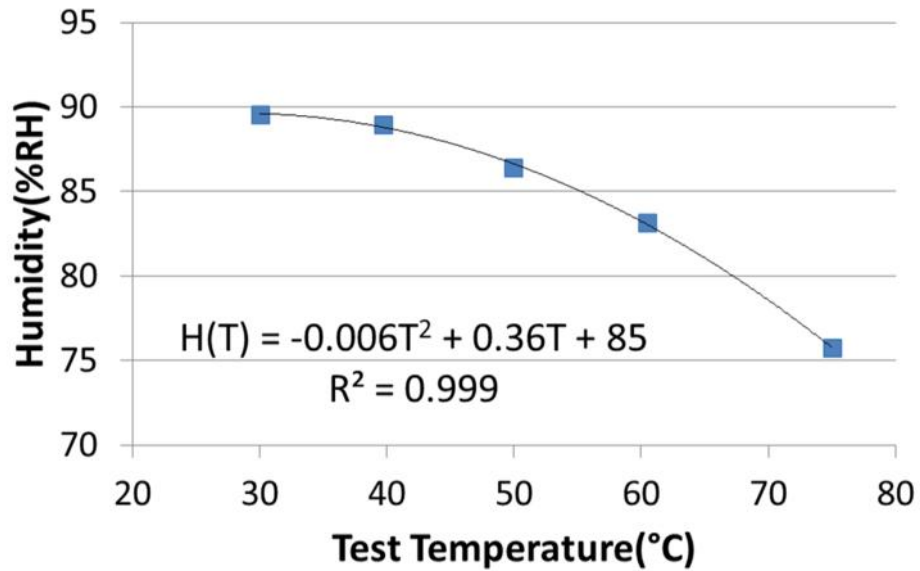
**Figure 14. Humidity as a function of Temperature**

$$H(T) = -0.006T^2 + 0.36T + 85$$
$$R^2 = 0.999$$



$$H(T) = -0.002T^2 - 0.1111T + 96.33$$
$$R^2 = 0.9625$$
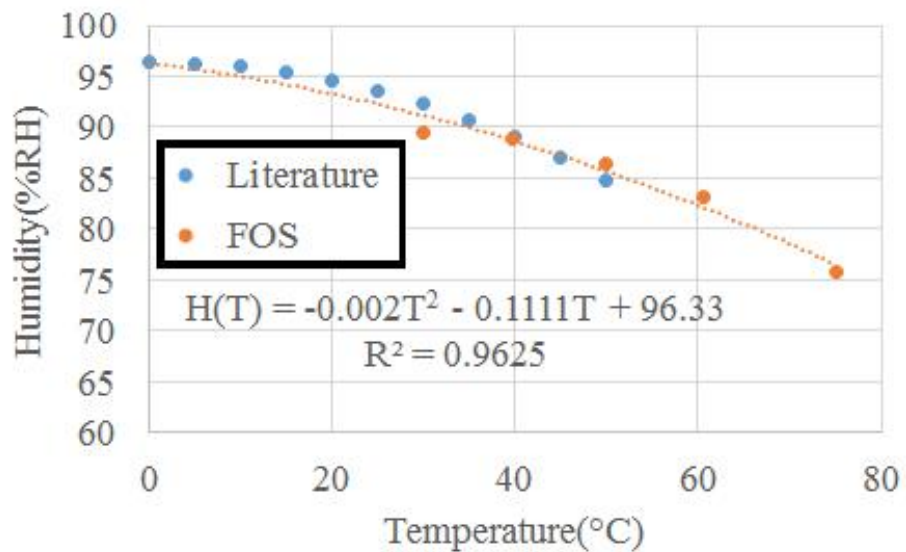
**Figure 15. Humidity data fit with data from [17]**

Further, higher temperatures cause a power law increase in the concentration of sulfur

vapor within the FOS test environment [18]. The linear relationship between

changing these two factors and the effect on corrosion is documented in the literature

for gas testing [6]. The literature also shows an expected power law relationship

between increasing test time in a controlled corrosive environment [3,5,8].

**Table 5. Relationships between Environmental Factors**

| Factor | Temperature Relationship | Corrosion Relationship |
|---|---|---|
| **Temperature** | --- | Exponential |
| **Humidity** | $2^{nd}$ order Polynomial | Linear (RH>60%) |
| **Sulfur Concentration** | Power | Linear |
| **Time** | --- | Power Law |

# Chapter 3: Experimental Setup

## *3.1 Test Samples*

Copper coupons test samples were used in the Flowers of Sulfur Testing. Coupons were made of Oxygen-Free High Conductivity Copper (OHFC). They were prepared as described in ASTM B810 [9]. A .5 mm thick copper sheet was cut into 12.5 mm by 12.5 mm squares. A 2.5 mm diameter hole was cut into each coupon in order to hang them. A schematic of a sample coupon can be seen in the figure below.
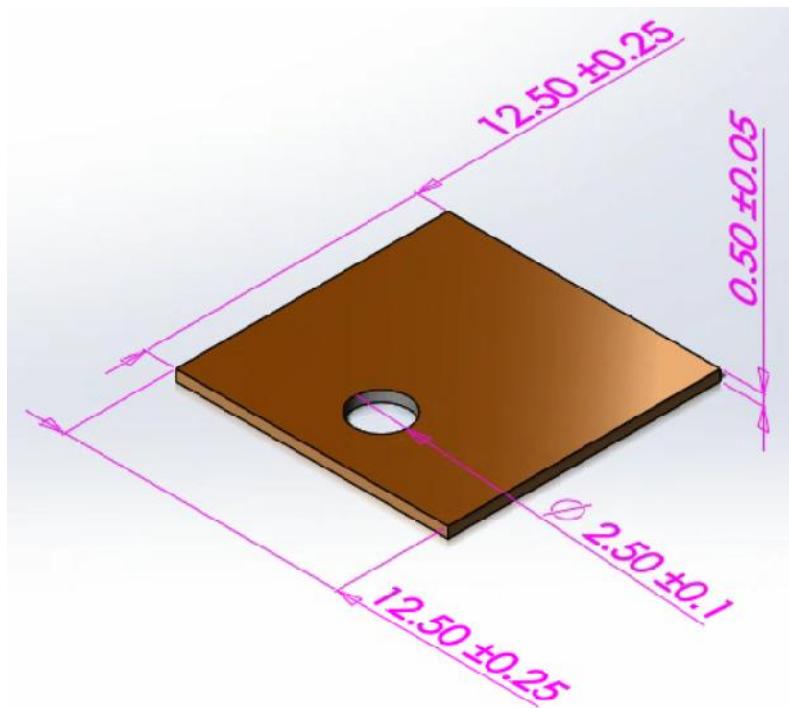


**Figure 16. Copper coupon Schematic (Dimensions in mm)**

Samples were cleaned prior to exposure in order to remove any surface oils, particulates, or oxide build up. Cleaning method 2 in ASTM B810 was used [9]. As

described in the method, coupons were cleaned by sequential rinses, with 10 second

drying periods in between. Coupons were first rinsed in n-Hexane for two minutes.

This was followed by a 15 second rinse in Alphametals Lonco Flux 3355-11. The

final steps in cleaning were two 15 second rinses in deionized water and a 15 second

rinse in methanol. After this cleaning, coupons were allowed to air dry for an hour

before being weighed. The table below summarizes the cleaning procedure.

**Table 6. Cleaning steps for copper coupons**

| Step | Fluid | Duration (Seconds) |
|------|-------|--------------------|
| 1 | n-Hexane | 120 |
| 2 | Air | 10 |
| 3 | Flux | 15 |
| 4 | Air | 10 |
| 5 | Deionized Water | 15 |
| 6 | Air | 10 |
| 7 | Deionized Water | 15 |
| 8 | Air | 10 |
| 9 | Methanol | 15 |
| 10 | Air | 60 |

Coupons were weighed before and after the Flowers of Sulfur exposure. Both before

and after the exposure the coupons were allowed to equilibrate for an hour as

described in the standard. Coupons were weighed three times each, with the reported

weight being an average of these three measurements. Weighing was done on a

microbalance with precision to a tenth of a milligram. Between each set of weight

measurements the microbalance was calibrated.

## 3.2 Flowers of Sulfur Setup

Flower of Sulfur (FOS) Testing was carried out as described in ASTM B809-95 [22].

A 10 liter glass desiccator was used as outlined in the standard. A saturated potassium

nitrate [>99%, Fisher Scientific] salt solution (200 g KNO3 in 200 mL H2O) was

placed in the bottom of the test vessel. Sublimed sulfur [Fisher Scientific] was placed

into a 15 cm diameter petri dish that was on top of the salt solution. The samples for

each test were suspended over the sulfur source in the center of the desiccator. Tests

were carried out by placing the test vessel in an oven [AH-205, BMA] until the

temperature measured using a thermocouple in the vessel reached the target

temperature. The figure below shows the FOS test vessel with samples.
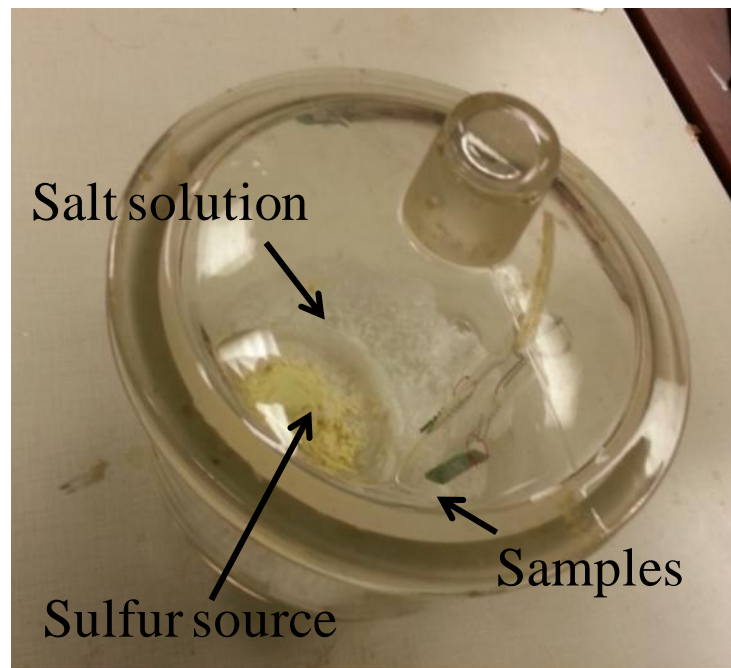


**Figure 17. FOS Test Vessel**

*3.3 Test Matrix*

The ASTM Flowers of Sulfur test as described in [22] is run at 50 degrees Celsius for a 24 hour duration. In order to increase the severity of the test environment, the duration of the test and the temperature of the oven were taken to elevated values. Tests were run at several elevated oven temperatures (75 °C, 85 °C, 95 °C, and 105 °C) in addition to the standard temperature (50 °C). The standard test duration (1 day) and extended duration (5, 10, and 15 day) tests were carried out. The complete test matrix can be seen in the figure below.

| Test Matrix | Duration (Days) | | | |
|---|---|---|---|---|
| Temperature (°C) | 1 | 5 | 10 | 15 |
| 50 | ■ | ■ | ■ | ■ |
| 75 | ■ | | ■ | |
| 85 | ■ | ■ | ■ | ■ |
| 95 | ■ | | ■ | |
| 105 | ■ | ■ | ■ | |

**Figure 18. Test Matrix (Tested Conditions Colored)**

# Chapter 4: Results

## *4.1 Corrosion Thickness Calculations*

The average copper coupon weight gain for each test condition was converted to copper corrosion film thickness. This was done using the surface area of the copper coupons and a known relationship between weight gain to thickness relationship (1 µg/cm2 = 89 Å as detailed in Appendix 1). This relationship assumes a copper sulfide corrosion film, and has been verified experimentally. The result of this calculation can be seen in Figure 19 and Figure 20. Both of these graphs are plotted on logarithmic scales in order to better represent the data. In both of these graphs there is overlap of test groups, especially at lower durations and temperatures. In order to verify that the different test groups were indeed statistically different, an ANalysis Of Variance Analysis(ANOVA) was carried out as described in the next section.
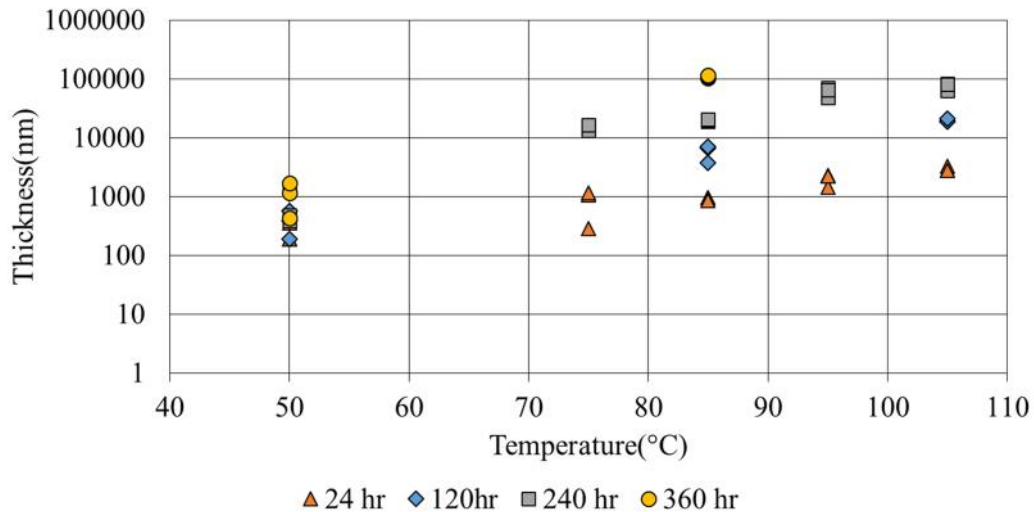


**Figure 19. Experimental results as a function of Temperature**

29
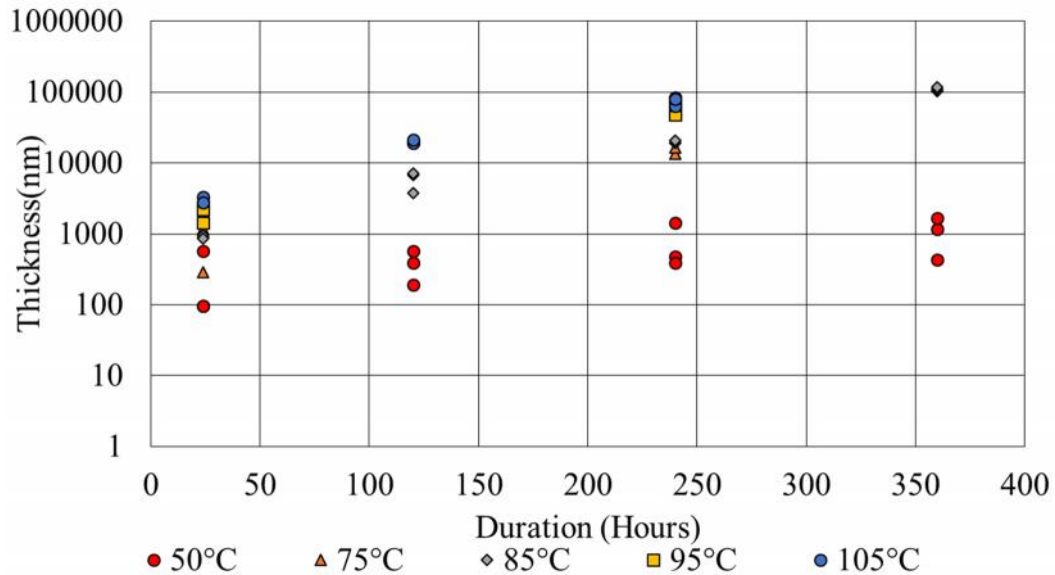
**Figure 20. Experimental Results as a function of Time**

*4.2 ANalysis Of VAriance(ANOVA) for Experimental Data*

An ANalysis Of Variance Analysis(ANOVA) was carried out for the different experimental test groups. F-tests were carred out, comparing each test group to each other test group. P-values were recorded, and a cutoff of .1 was used in the following analysis. The data can be seen in Table 7 (a larger version is in Appendix 3). Highlighted values are p-values greater than the .1 cutoff.



**Table 7. P-Values for ANOVA Analysis (P-values>.1 are Highlighted)**

The data for the tests at each temperature were compared to each other test at that temperature, as seen in Table 8. It can be observed that for each test above 50ºC, the

different tests appeared to be distinct based on variance. The natural conclusion for this is that the lower temperature test (in this case the 50ºC test) resulted in less discernable corrosion. However, as seen in the table, a comparison of the 15 day and 1 day tests at 50 ºC had a p-value that was deemed as acceptable. For the 50ºC test condition, caution should be made with regards to tests shorter than 15 days.

| P values | | 50C | | | |
|---|---|---|---|---|---|
| | | 1 day | 5 day | 10 day | 15 day |
| 50C | 1 day | | 3.28E-01 | 2.01E-01 | 8.28E-02 |
| | 5 day | 3.28E-01 | | 3.40E-01 | 1.36E-01 |
| | 10 day | 2.01E-01 | 3.40E-01 | | 5.53E-01 |
| | 15 day | 8.28E-02 | 1.36E-01 | 5.53E-01 | |

| P values | | 75C | |
|---|---|---|---|
| | | 1 day | 10 day |
| 75C | 1 day | | 1.21E-03 |
| | 10 day | 1.21E-03 | |

| P values | | 85C | | | |
|---|---|---|---|---|---|
| | | 1 day | 5 day | 10 day | 15 day |
| 85C | 1 day | | 1.01E-02 | 5.74E-06 | 8.70E-06 |
| | 5 day | 1.01E-02 | | 3.49E-04 | 1.23E-05 |
| | 10 day | 5.74E-06 | 3.49E-04 | | 1.96E-05 |
| | 15 day | 8.70E-06 | 1.23E-05 | 1.96E-05 | |

| P values | | 95C | |
|---|---|---|---|
| | | 1 day | 10 day |
| 95C | 1 day | | 1.02E-03 |
| | 10 day | 1.02E-03 | |

| P values | | 105C | | |
|---|---|---|---|---|
| | | 1 day | 5 day | 10 day |
| 105C | 1 day | | 1.07E-05 | 3.34E-04 |
| | 5 day | 1.07E-05 | | 9.33E-04 |
| | 10 day | 3.34E-04 | 9.33E-04 | |

**Table 8. ANOVA Results - Fixed Temperature (p-values)**

The data for the tests carried out for each duration was also examined in detail. As seen in Table 9, there were two places where the tests could not be seen as different based on variance. For the lower temperature tests (<95ºC) that were within 25º of each other, the p-values were greater than the .1 cutoff. This is consistent with the idea that at lower durations and lower temperatures the variance of the corrosion process could be the large enough to affect the results of the test. A similar issue is seen in the 10 day tests at higher temperatures.

| P values | | 1 Day | | | | |
|---|---|---|---|---|---|---|
| | | 50C | 75C | 85C | 95C | 105C |
| 1 Day | 50C | | 1.04E-01 | 4.17E-04 | 3.37E-03 | 1.05E-04 |
| | 75C | 1.04E-01 | | 7.45E-01 | 4.08E-02 | 2.78E-03 |
| | 85C | 4.17E-04 | 7.45E-01 | | 1.85E-02 | 2.90E-04 |
| | 95C | 3.37E-03 | 4.08E-02 | 1.85E-02 | | 4.14E-02 |
| | 105C | 1.05E-04 | 2.78E-03 | 2.90E-04 | 4.14E-02 | |

| P values | | 5 Day | | |
|---|---|---|---|---|
| | | 50C | 85C | 105C |
| 5 Day | 50C | | 7.12E-03 | 5.61E-06 |
| | 85C | 7.12E-03 | | 3.46E-04 |
| | 105C | 5.61E-06 | 3.46E-04 | |

| P values | | 10 Day | | | | |
|---|---|---|---|---|---|---|
| | | 50C | 75C | 85C | 95C | 105C |
| 10 Day | 50C | | 1.28E-03 | 9.74E-06 | 9.43E-04 | 2.99E-04 |
| | 75C | 1.28E-03 | | 3.84E-02 | 1.41E-02 | 5.23E-03 |
| | 85C | 9.74E-06 | 3.84E-02 | | 3.86E-03 | 9.28E-04 |
| | 95C | 9.43E-04 | 1.41E-02 | 3.86E-03 | | 2.01E-01 |
| | 105C | 2.99E-04 | 5.23E-03 | 9.28E-04 | 2.01E-01 | |

| P values | | 15 Day | |
|---|---|---|---|
| | | 50C | 85C |
| 15 Day | 50C | | 8.92E-06 |
| | 85C | 8.92E-06 | |

**Table 9. ANOVA Results - Fixed Duration (p-values)**

A comparison of fixed temperature and duration tests to the baseline (50ºC for 1 day) is seen in Table 10. In order to reach a test that was discernable from the standard test, the temperature had to be raised to 85ºC for a 1 day test.

| P values | | 1 Day | | | | |
|---|---|---|---|---|---|---|
| | | 50C | 75C | 85C | 95C | 105C |
| 50C | 1 day | | 1.04E-01 | 4.17E-04 | 3.37E-03 | 1.05E-04 |
| | 5 day | 3.28E-01 | 2.04E-01 | 9.21E-03 | 5.60E-03 | 2.17E-04 |
| | 10 day | 2.01E-01 | 8.90E-01 | 6.61E-01 | 4.87E-02 | 4.51E-03 |
| | 15 day | 8.28E-02 | 6.02E-01 | 6.82E-01 | 1.19E-01 | 9.78E-03 |

**Table 10. ANOVA Results - Baseline Comparison**

*4.3 Corrosion Thickness as a Function of Temperature*

A variety of fits were examined for the corrosion film thickness as a function of temperature. Table 11 shows the $R^2$ for these fits for the 1 Day and 10 Day data sets. These two data sets were used as they were the only complete ones. Looking at the table, it is clear that an exponential fit for temperature had the best fit.

**Table 11. Corrosion fits for temperature**

| Function | $R^2$(1 Day) | $R^2$ (10 Day) | $R^2$ (avg) |
|---|---|---|---|
| Linear | 0.834 | 0.82 | 0.827 |
| Power | 0.963 | 0.962 | 0.962 |
| Exponential | 0.980 | 0.956 | **0.968** |
| Logarithmic | 0.750 | 0.740 | 0.745 |
| Polynomial(2nd) | 0.978 | 0.946 | 0.962 |
| Sum of Sines | 0.833 | 0.818 | 0.825 |

Assuming that the direct temperature effect is dominant, corrosion film thickness for a fixed duration can be written as equation 2, agreeing with the exponential fit. For

the FOS test environment, the temperature effect on corrosion film thickness was able

to be modeled using this relationship that comes from the effect of temperature

increasing reaction rate. An exponential fit for the 1 day test duration has a high

correlation with experimental data ($R^2$ = .98) as does the 10 day test duration($R^2$ =

.96) as seen in Figure 21. Increasing the temperature of the FOS test environment

increased corrosion film thickness, meaning that the corrosivity of the FOS can be

increased. Harsher testing environments lead to reduced testing time when using the

FOS for part screening. Equation 2 shows corrosion film thickness ( ) [in nm] as a

function of temperature (T) [in °C].

$$ = e^{BT} \qquad [2]$$
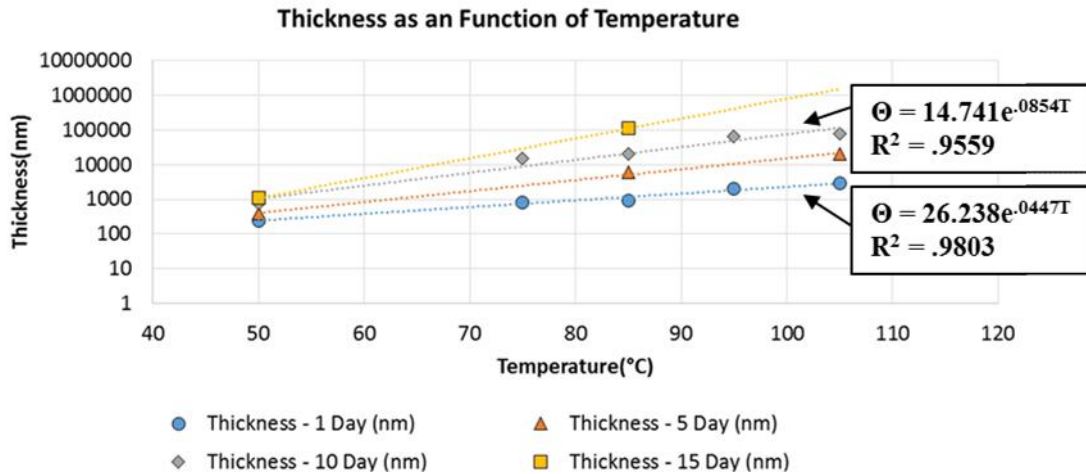


**Figure 21. Corrosion Film Thickness as a Function of Temperature**

In order to examine the accuracy of using an exponential fit to extraplote for the

expected values at higher temperatures, additional analysis was carried out. The value

at the 105°C temperature was estimated using an exponential fit that only used the

lower temperatures. This was done using the 1 day and 10 day data sets. The result of

this fitting, and the minimum and maximum experimental measurements are seen in Figure 22 and Table 12. The initial-value fit using temperature is good for the 1 day data sets, but not as good for the 10 day data set. In the 10 day data set, the fit overestimates the amount of corrosion. This may hint that there is something, such as a diffusion-limit that reduces the amount of corrosion in cases where the corrosion film is thicker.

**Thickness as an Function of Temperature**

$$\Theta = 7.3598e^{.0958T}$$
$$R^2 = .9744$$

$$\Theta = 27.575e^{.0439T}$$
$$R^2 = .9688$$

Used for fit     Min/Max(experimental)

- ● 1 Day ■ 10 Day ◆ 1 Day ◆ 10 Day
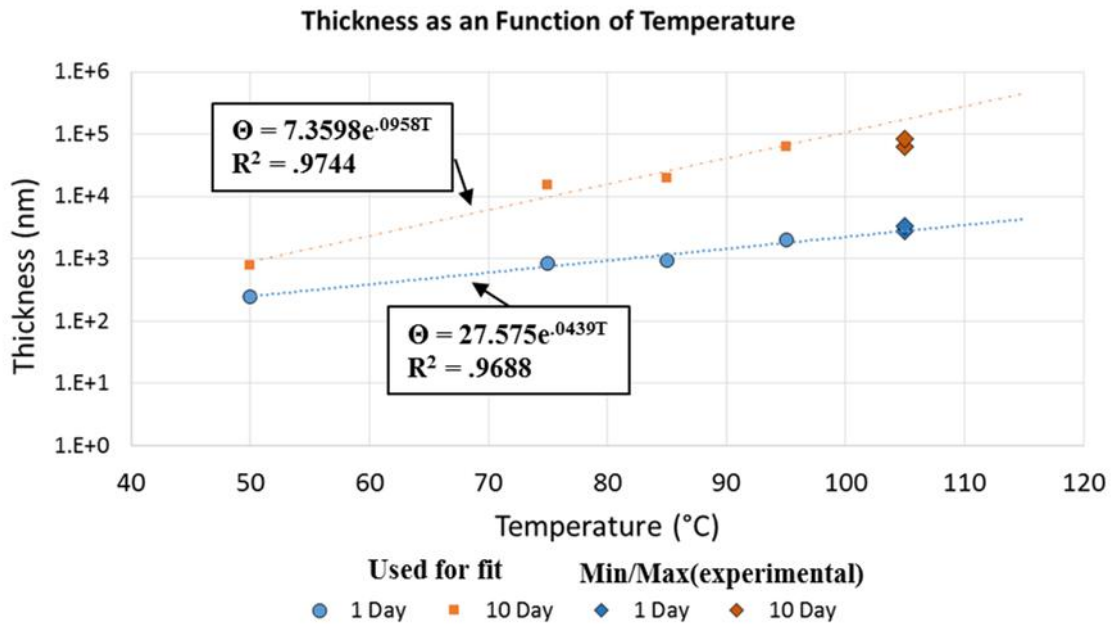
**Figure 22. Initial-value temperature fits**

**Table 12. Data for initial-value temperature fits**

|  | Expected | Actual | |
| --- | --- | --- | --- |
|  | Calculated | Min | Max |
| 1 Day | 2769.5 | 2762 | 3279 |
| 10 Day | 171962 | 63772 | 84850 |

## 4.4 Corrosion Thickness as a Function of Time

A variety of fits were examined for the corrosion film thickness as a function of time as well. Table 13 shows the $R^2$ for these fits for the 50°C and 85°C data sets. These two data sets were used as they were the only complete ones. Looking at the table, it is clear that an exponential fit for time had the best fit.

**Table 13. Corrosion fits for time**

| Function | R²(50C) | R²(85C) | R² avg |
|---|---|---|---|
| Linear | 0.985 | 0.773 | 0.879 |
| Power | 0.905 | 0.926 | 0.915 |
| Exponential | 0.983 | 0.987 | **0.985** |
| Logarithmic | 0.796 | 0.480 | 0.638 |
| Polynomial(2nd) | 0.992 | 0.977 | 0.984 |
| Sum of Sines | 0.985 | 0.268 | 0.626 |

Theoretically, the time term is could fit a power law based on the literature for a diffusion controlled corrosion process [34]. However, as shown in Table 13, a power law does not provide a good fit for the FOS test data. Instead, an exponential fit is much more suitable as seen in Figure 23 ($R^2$=.98 for 50C, $R^2$=.99 for 85C). This may be because the corrosion in the FOS may not reach a diffusion-limited state within the 15 day duration that was the maximum duration for this study. The exponential relationship with time may hint at an autocatalytic effect for corrosion in the FOS, but further investigation is needed. Looking at Figure 23, we can see that the model, when extrapolated to time equal to zero, gives a value for corrosion thickness. This

inconsistency with the actuality of no film formation at time equals zero cautions

against extrapolating this model for time less than 24 hours.



$$\Theta = 821.28e^{.0137t}$$
$$R^2 = .9867$$

$$\Theta = 238.33e^{.0044t}$$
$$R^2 = .9839$$
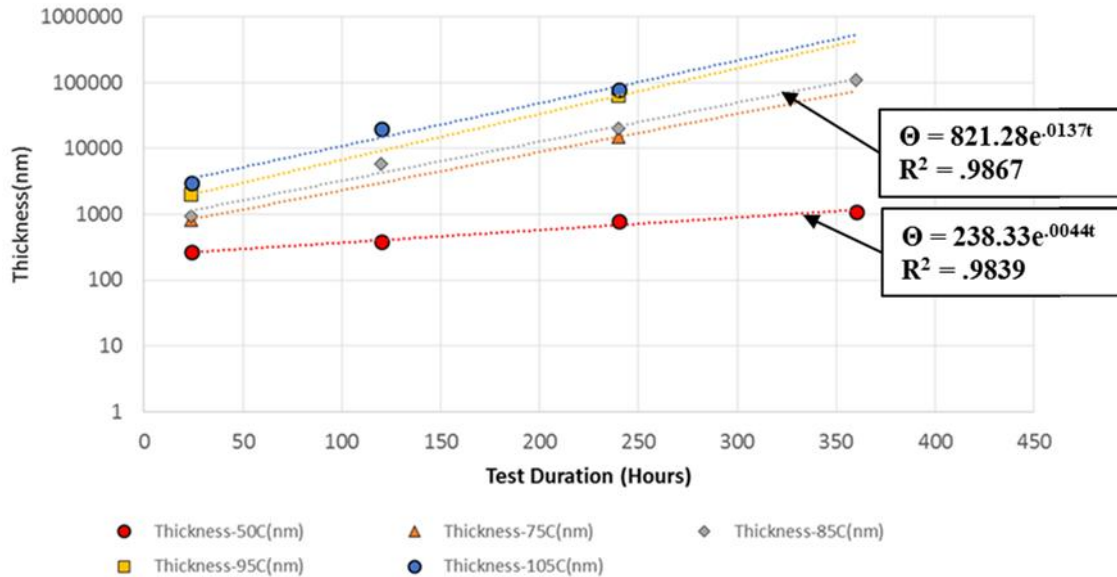
**Figure 23. Corrosion Film Thickness as an exponential function of time.**

Additional analysis was carried out similar to the high temperature analysis in order

to examine the accuracy of using an exponential fit to extraplote for the expected

values at higher test durations. The corrosion film thickness at the 15 day duration

was estimated using an exponential fit that only used the lower duration tests. This

was done using the 50°C and 85°C data sets. The result of this fitting, and the

minimum and maximum experimental measurements are seen in Figure 22 and Table

12. The initial-value fit using time is good for the 50°C data set, but not as good for

the 85°C data set. In the 85°C data set, the fit slightly overestimates the amount of

corrosion. This may hint that there is something, such as a diffusion-limit that reduces

the amount of corrosion in cases where the corrosion film is thicker.

Thickness as a Function of Time

$\Theta = 797.7e^{.014t}$
$R^2 = .9668$

$\Theta = 213.13e^{.00t}$
$R^2 = .9961$

Used for fit    Min/Max(experimental)
● 50 °C    ■ 85 °C    ◆ 50 °C    ◆ 85 °C
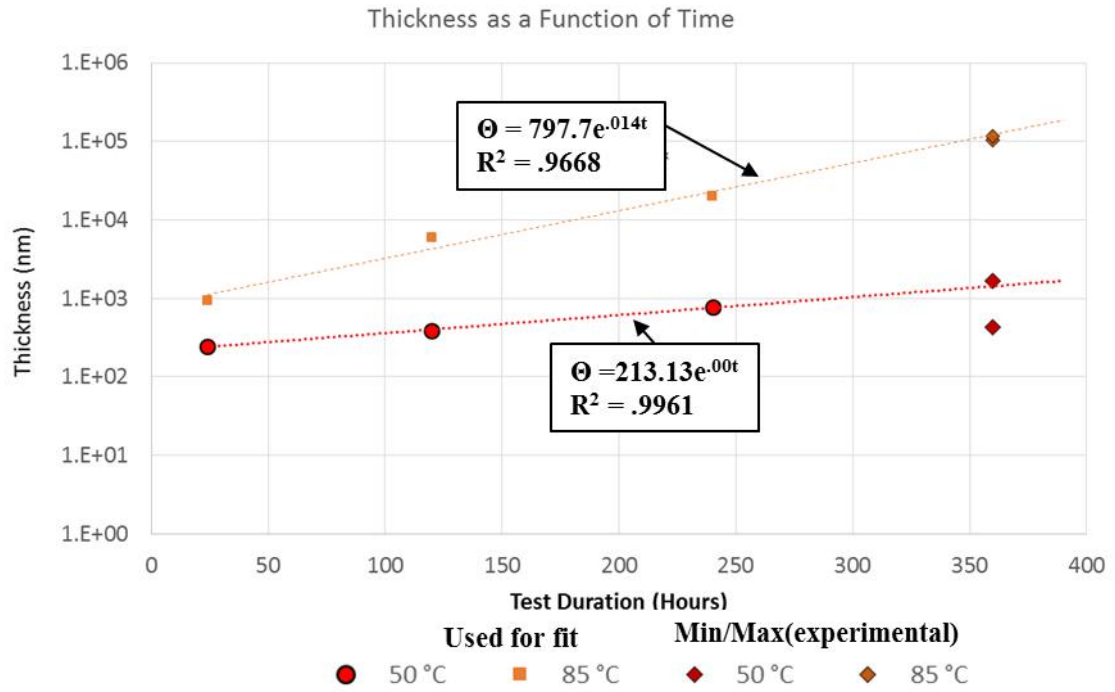
**Figure 24. Initial-value time fits**

**Table 14. Data for initial-value temperature fits**

|  | Expected | Actual | |
|---|---|---|---|
|  | Calculated | Min | Max |
| 50°C | 1436 | 434 | 1688 |
| 85°C | 123221 | 102814 | 115835 |

For shorter duration tests, this exponential fit is not needed. One and five day data for

the 85°C and 105°C could be fit using a linear fit as seen in Figure 25. Linear models

are commonly used for the first stage of some corrosion process [4] [6] [34]. The data

for the 50°C test was not included as the effect of variance was too great as discussed

earlier.
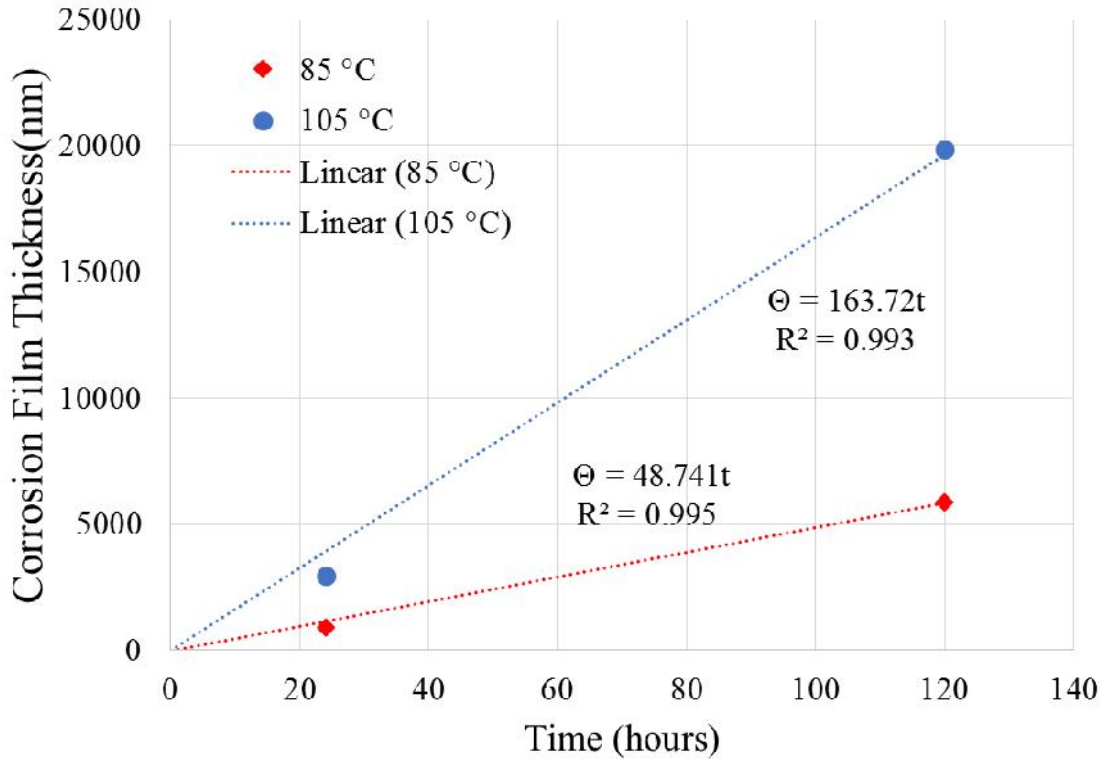
**Figure 25. Linear fits for low-duration data**

*4.5 Comparison of Experimental and Theoretical Corrosion Rates*

As detailed above, the corrosion thickness in the FOS can be experimentally modeled as an exponential function. This experimental rate can be compared to a theoretical reaction rate for the formation of copper sulfide. Possible processes that will be considered are summarized in Table 15. These are summaries as there are multiple ways that the reactants can lead to the products (For example, the breakdown of sulfur can go through a variety of different sulfur vapors).

**Table 15. Summary reactions for FOS**

| Reaction | Summary |
|---|---|
| Oxidation of Copper | $Cu_{(m)} \quad Cu^+ + e^-$ |
| Breakdown of Sulfur | $S_8 \quad S^{2-}$ |
| Formation of Copper Sulfide | $2\ Cu^+ + S^{2-} \quad Cu_2S$ |

39

Several assumptions must be made in order to identify a rate-limiting factor based on these processes. The first is that the oxidation of copper metal is uninhibited by the formation of the copper sulfide film. This assumption can be made as the experimental data showed no drop-off in corrosion rate. If the corrosion film inhibited the creation of copper ions, there would be a terminal thickness after which no copper could be accessed. Within the time frame of this paper, it appears this phenomenon is not dominant. Another major assumption that can be made is that the breakdown at sulfur is not limited. In the vapor region of the FOS, sulfur vapor can exist in a variety of states ($S_8$, $S_7$, $S_6$, $S_5$, $S_4$, $S_3$, or $S_2$,). If can be assumed that these vapor states find an equilibrium at a fixed temperature, such as in the FOS [35]. If it is assumed that this equilibrium in the vapor is maintained with the equilibrium in the water layer formed on the copper, then we can ignore the possibility that the breakdown of sulfur is the rate-controlling factor. Looking at the Table 15, we can see that eliminating the oxidation of copper and the breakdown of sulfur as controlling factors leaves the formation of copper sulfide as the expected rate-limiting factor. Reaction rates for copper and sulfur-containing contaminants are assumed to be constant for fixed environments in the literature [6-8]. Based on the concentration of sulfur and other parameters, the rate can be seen to vary from .002-4.08 $\mu g/cm^2$–hr in MFG laboratory tests described in [6]. In the FOS test results in this thesis, corrosion rates were 1.15-35.9 $\mu g/cm^2$–hr. FOS testing resulted in higher corrosion rates than those typical in the literature as those atmospheric tests are not carried out at elevated temperatures. Constant corrosion rates presented in the literature would be expected to lead to corrosion being a linear function of time [8]. However, this is not the case

in the FOS. This may be because the concentration of sulfur available for reaction in the water layer formed in the FOS changes as a function of time. Additional testing would need to be carried out to confirm this hypothesis.

*4.6 Corrosion Modeling for the Flowers of Sulfur Test Environment*

Combining the exponential relationship for temperature and the exponential relationship for test duration, equation 3 is created for corrosion film thickness ( ) [in nm] as a function of temperature (T) [in °C] and time (t) [in hours]

$$ = X(e^{YT} * e^{Zt}) \qquad\qquad [3]$$

Fitting the experimental data to this model, values can be found for the coefficients (X=4.27e10, Y=50583, Z=.0114). This model has a very strong correlation coefficient ($R^2$ = .951).
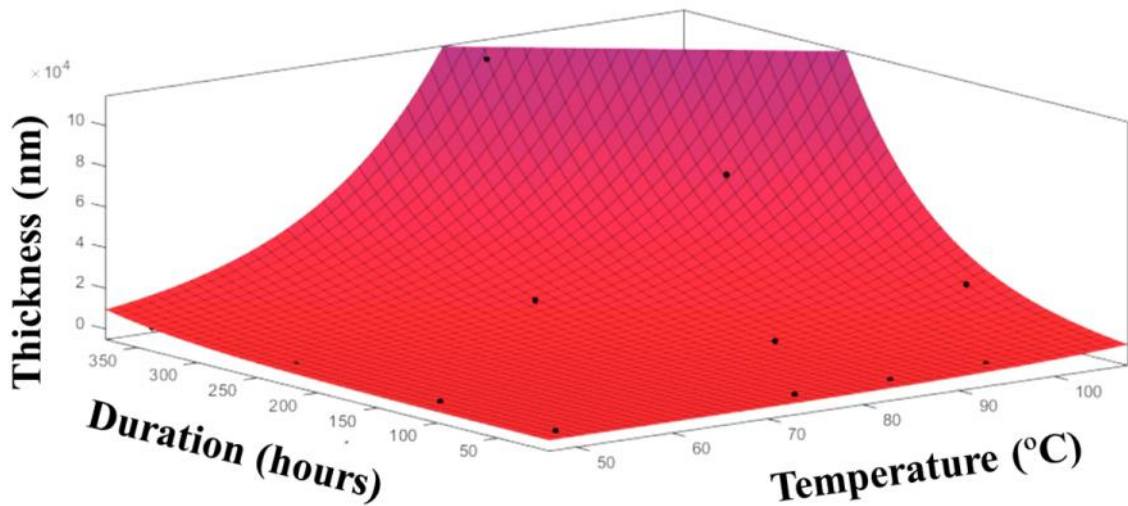


**Figure 26. Model for film thickness as a function of time and temperature**

The two-parameter model for corrosion film thickness that is both an exponential temperature and test duration seems to be a good fit when looking at the wide span of experimental data. However, when we examine the theoretical implications of extending such a model, we find that there are obvious issues with assuming that the model captures all effects at its boundaries.  If we calculate the derivative with respect to time assuming a fixed temperature, we find that $d\delta/dt = XZe^{YT}(e^{Zt})$. As t increases, the corrosion film thickness increases exponentially. As we know that there is a maximum amount of corrosion that can occur on the coupon, we know that this is a problem. Similarly, taking the derivative with respect to temperature with a constant duration we can find $d\delta/dT = XYe^{Zt}(e^{YT})$. As test temperature increases, the corrosion film thickness increases exponentially as well. This too is in conflict with the idea of a maximum amount of corrosion in the FOS.

### *4.7 Applying the two-parameter model for FOS testing*

This two-parameter model for FOS testing can be used to determine what test conditions to use based on expected field conditions. Figure 27 shows the process for using the method provided in Appendix 4.
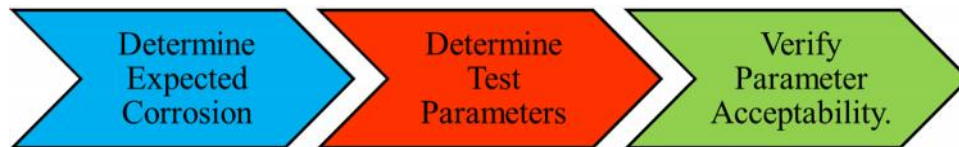


**Figure 27. Process for applying the 2-parameter FOS model**

The first step is to quantify the corrosion rate from field conditions. In this case, let us say that coupons place into our field environment gained 20 nm/month. The expected

42

corrosion can be calculated as a result of a life time. For this case study, let us say that

our part should last 15 years and that the corrosion growth is linear. This would make

us set our expected film thickness, $\quad$ = 15yr x 12mo/yr x 20nm/mo = 3600 nm.

The next step is to select test parameters to fix. For this case study, let us say that we

would like to have tests at 60°C, 80°C, and 100°C. Using the fixed parameters, find

the other test parameter. In this case, we use equation 4 with $\quad$ =3600 nm, and T set

to 60°C, 80°C, and 100°C. Using these parameters, we find test times of 236, 129,

and 22 hours respectively.

 The final step is for each test condition set, todetermine if it satisfies the limitations

in the application notes. Looking at the notes, we see that the 100°C is below the

minimum duration (22 hours<24 hour minimum). This means that while the 60°C or

80°C test would be fine, a 100°C test using the FOS is not recommended.

# Chapter 5:  Conclusions

## *5.1 Contributions*

The major contribution of this thesis was the development of a model for the effects of increased temperature and test time on copper corrosion rates of the FOS test. This model can be used to control the FOS test environment, based on target field environment and expected exposure period for durations up to 15 days and temperatures from 50°C to 105°C.

In order to create this model, two experimental relationships for the FOS were examined. The work in this thesis established that increasing test temperature in the FOS environment can be modeled by an exponential function from 50°C to 105°. It was also determined that the effect of test duration on the FOS can be modeled by an exponential function for the first 15 days. The corrosion process is concentration-limited.

## *5.2 Summary of Results*

Flowers Of Sulfur (FOS) Testing at higher temperatures and for longer durations that those outlined in ASTMB809 has been shown to increase the amount of corrosion creating in the FOS test environment. Both parameters have been shown to be able to increase the amount of corrosion observed on copper coupons by orders of magnitude. High temperature testing using the FOS can increase the acceleration of laboratory corrosion tests, resulting in shorter test durations. This elevated corrosion rate can result in higher test throughput, which is valuable for component and device manufacturers for whom the FOS serves as a suitable test environment. Longer

duration testing has been shown to increase the amount of corrosion seen in a non-linear manner. While this is very interesting finding, it is important to note that this may not be applicable for corrosion processes where the reaction is material limited.

This thesis demonstrated that a two parameter model can be used to model the corrosion rate in the FOS test environment. An exponential term is able to handle the effect of the temperature effect. Another exponential relationship is able to capture the effect of increasing the duration of the test for the different temperatures. This model is useful as a guideline for how the conditions of the FOS test can be changed to increase the corrosivity of the test environment. This should prove to be a valuable tool for the adaptation of the FOS test for component testing.

## *5.3 Future Work*

The work presented in this thesis provides the opportunity for additional testing that can be used to expand understanding of the Flowers of Sulfur test environment. As explained earlier, the exponential time term for this model does not allow for extrapolation below the 24 hours that was the minimum tested duration. Investigation of the FOS test at lower temperatures could be useful in expanding the lower bounds of this model. It is also possible that including other parameters such as humidity and concentration in the model may be able to adjust the model to solve this issue.

As discussed in previous sections, the single parameter models overestimate corrosion at higher temperatures and test durations. At these places, it is also the case

that the corrosion film is the thickest. It is expected that as the corrosion film thickness grows the ability to attack the underlying copper is restricted. However, the experimental data in this thesis did not show the power law relationship expected if this is the case. The model presented did have some issues with the edges of the boundary conditions, however not enough data has been gathered to create a model that also captures this effect. Additional, longer duration tests and higher temperature would need to be carried out to capture this effect.

Different salt solutions change the relative humidity as a function of temperature. Attempting to use this model for a different salt solution could demonstrate the effect of humidity on the FOS test. Alternatively, changing the surface area of the sulfur in the chamber should change the amount of corrosion. A series of studies could look at how exposed sulfur affects the thickness model.

# Appendices

*Appendix 1: Converting copper coupon weight gain to corrosion film thickness*

Weight gain of copper coupons in a corrosive environment can be converted to film thickness using the information provided in Table 16.

**Table 16. Material Properties for Cu, S, and Cu$_2$S**

| Property | Value |
|---|---|
| Atomic Weight – Cu | 63.6 |
| Atomic Weight - S | 32.0 |
| Density - Cu$_2$S | 5.6 g/cm$^3$ |

Using the data in the above table, the following conversions can be made:

Copper mass gain of 1 µg $\quad = \quad$ (2(63.6)+32.0)/32.0 µg of Cu$_2$S

$\qquad\qquad\qquad\qquad\qquad = \quad$ 4.97 * 10$^{-6}$ g of Cu$_2$S

$\qquad\qquad\qquad\qquad\qquad = \quad$ (4.97 * 10$^{-6}$ g)/(5.6 g/cm$^3$)

$\qquad\qquad\qquad\qquad\qquad = \quad$ .89* 10$^{-6}$ cm$^3$ of Cu$_2$S

Thus, for a normalized gain per unit area:

Copper mass gain of 1 µg/ cm$^2$ $\quad = \quad$ .89* 10$^{-6}$ cm of Cu$_2$S

$\qquad\qquad\qquad\qquad\qquad = \quad$ 89 Å of Cu$_2$S

Weight gain and thickness data for the different Flowers of Sulfur test conditions can be found in the tables below. Table 17 below shows normalized weight gain averages for samples placed in each test condition.

**Table 17. Normalized weight gain for the FOS tests**

| Normalized Weight Gain (mg/g) | | Test Duration (Days) | | | |
|---|---|---|---|---|---|
| | | **1** | **5** | **10** | **15** |
| **Temperature (°C)** | **50** | 0.130 | 0.190 | 0.395 | 0.565 |
| | **75** | 0.415 | | 0.760 | |
| | **85** | 0.468 | 2.903 | 9.805 | 54.082 |
| | **95** | 0.986 | | 32.032 | |
| | **105** | 1.451 | 9.964 | 38.146 | |

Table 18 below shows the average initial weight for each of the FOS test conditons which was used in calculating the film thickness.

**Table 18. Average Initial Weight for the FOS tests**

| Initial Weight (g) | | Test Duration (Days) | | | |
|---|---|---|---|---|---|
| | | **1** | **5** | **10** | **15** |
| **Temperature (°C)** | **50** | 0.697 | 0.703 | 0.675 | 0.669 |
| | **75** | 0.694 | | 0.706 | |
| | **85** | 0.688 | 0.702 | 0.698 | 0.698 |
| | **95** | 0.698 | | 0.679 | |
| | **105** | 0.702 | 0.688 | 0.695 | |

Table 19 below shows the average initial weight for each of the FOS test conditons which was used in calculating the film thickness. This was calculated using the data from Table 17, Table 18, and Table 19.

**Table 19. Corrosion Film Thickness for the FOS tests**

| Corrosion | Test Duration (Days) |
|---|---|

| Thickness (nm) | | 1 | 5 | 10 | 15 |
|---|---|---|---|---|---|
| **Temperature (°C)** | 50 | 263 | 386 | 772 | 1093 |
| | 75 | 833 | | 1552 | |
| | 85 | 932 | 5896 | 19788 | 109152 |
| | 95 | 1990 | | 62953 | |
| | 105 | 2948 | 19843 | 76758 | |

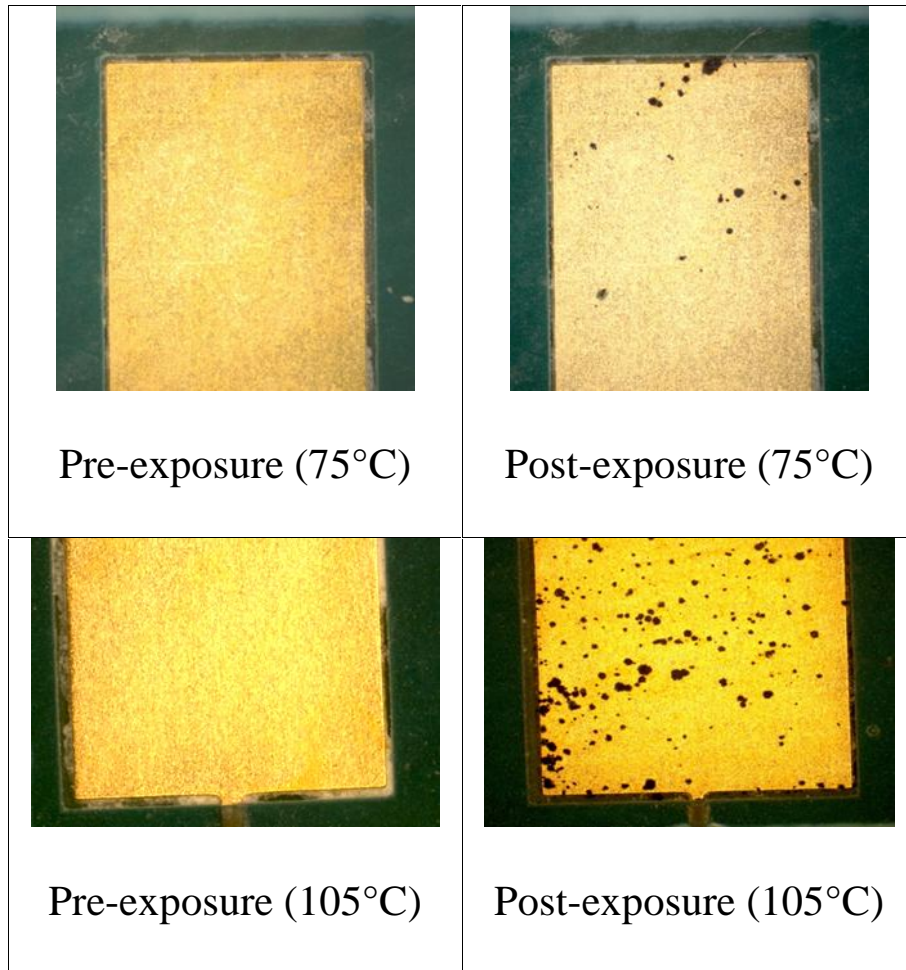*Appendix 3: Corrosion in High Temperature Flowers of Sulfur Test Conditions*

High Temperature Flowers of Sulfur test environments are useful in corrosion testing of electronics. The higher temperature creates a harsher test environment, which us useful for screening or identifying the failure site. Two Flowers of Sulfur tests were run at different conditions. A 12 day test was done at 75 °C (.8 mg/g Copper Coupon Weight Gain) and a 10 day test was done at 105 °C (39.4 mg/g Copper Coupon Weight Gain). Table 20 summarizes the two test conditions.

**Table 20. FOS Test Conditions for part testing**

| Test | Duration (Days) | Temperature (°C) | Weight Gain (mg/g) |
|------|-----------------|------------------|--------------------|
| A | 12 | 75 | .8 |
| B | 10 | 105 | 39.4 |

Several surface finishes were placed into these test environments in order to examine how increasing the test temperature of the FOS increased the amount of corrosion observed. Boards plated with Electroless Nickel Electroless Palladium Immersion Gold (ENEPIG), Immersion Silver (ImAg), and Organic Solder Preservative (OSP) were placed into the two test environments. Also, mounted chip resistors were placed into the two test environments.

Figure 28 below shows that the increase in temperature did not appear to affect the amount of corrosion observed on ENEPIG plated copper. Figure 29 shows that the temperature increase did not appear to change the amount or presence of corrosion on ImAg finish boards either.

|  |  |
|---|---|
| Pre-exposure (75°C) | Post-exposure (75°C) |
| Pre-exposure (105°C) | Post-exposure (105°C) |

**Figure 28. ENEPIG boards in high temperature FOS tests**



|  |  |
|---|---|
| Pre-exposure (75°C) | Post-exposure (75°C) |

| Pre-exposure (105°C) | Post-exposure (105°C) |
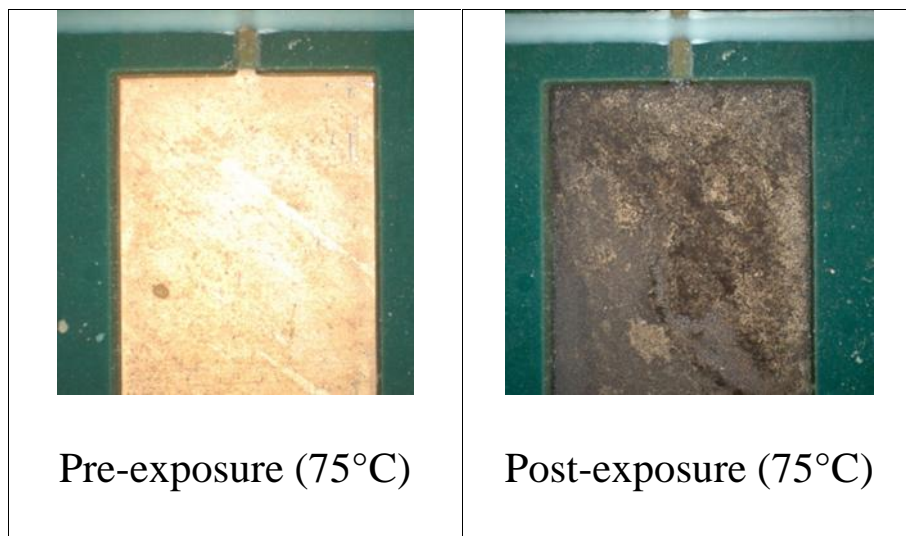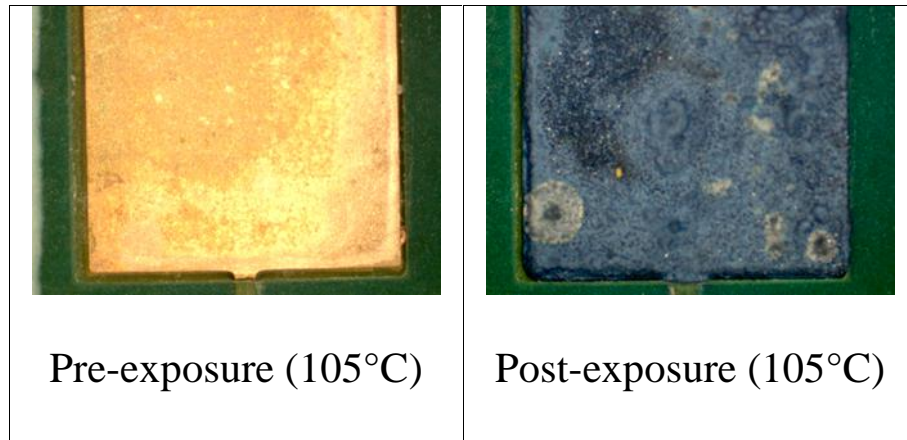
**Figure 29. ImAg boards in high temperature FOS tests**

However, increasing the temperature of the FOS test did have an effect on the corrosion of OSP finished boards. As seen in Figure 30, increasing the temperature of the FOS increased the amount of corrosion observed. These results are consistent with the fact that OSP breaks down at high temperatures.



| Pre-exposure (75°C) | Post-exposure (75°C) |

| Pre-exposure (105°C) | Post-exposure (105°C) |
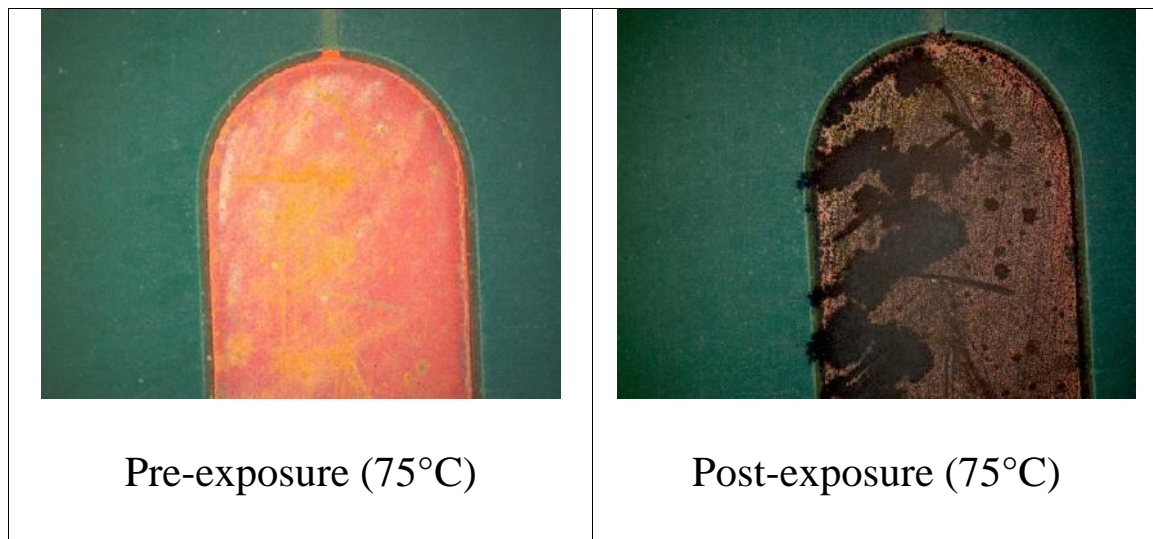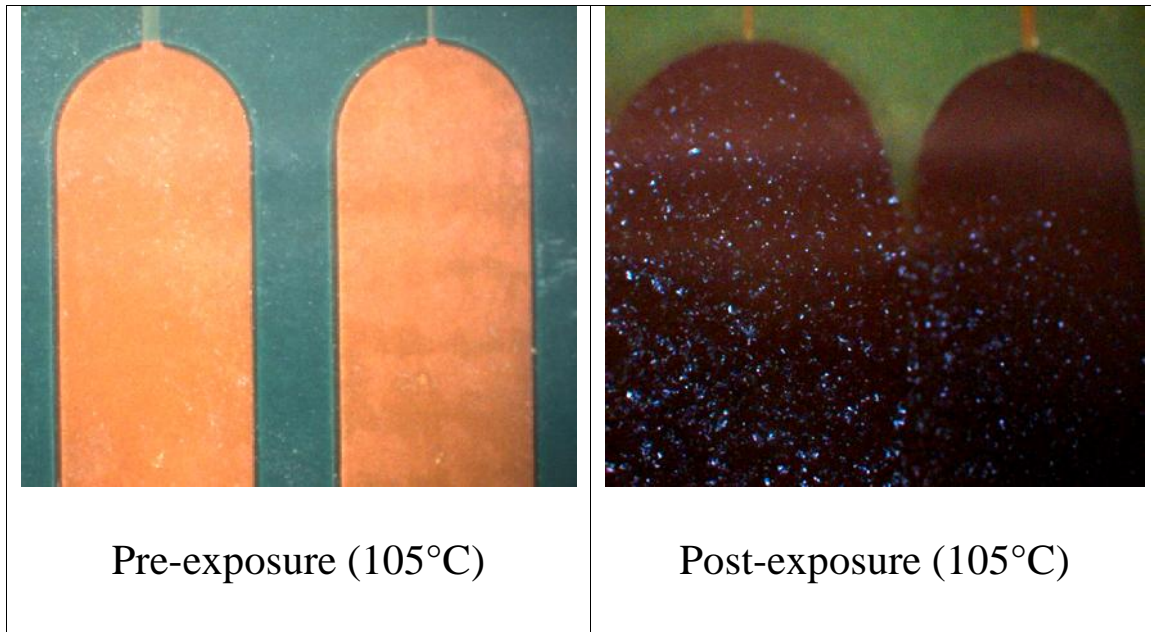
**Figure 30. OSP boards in high temperature FOS tests**

Increasing the temperature of the FOS test also had an effect on the corrosion of chip resistors. As seen in sdasd, increasing the temperature of the FOS increased the amount of corrosion observed. The outgrowths were confirmed to be silver sulfide using Energy Dispersive Spectroscopy (EDS).



| Post-exposure (75°C) | Post-exposure (75°C) |
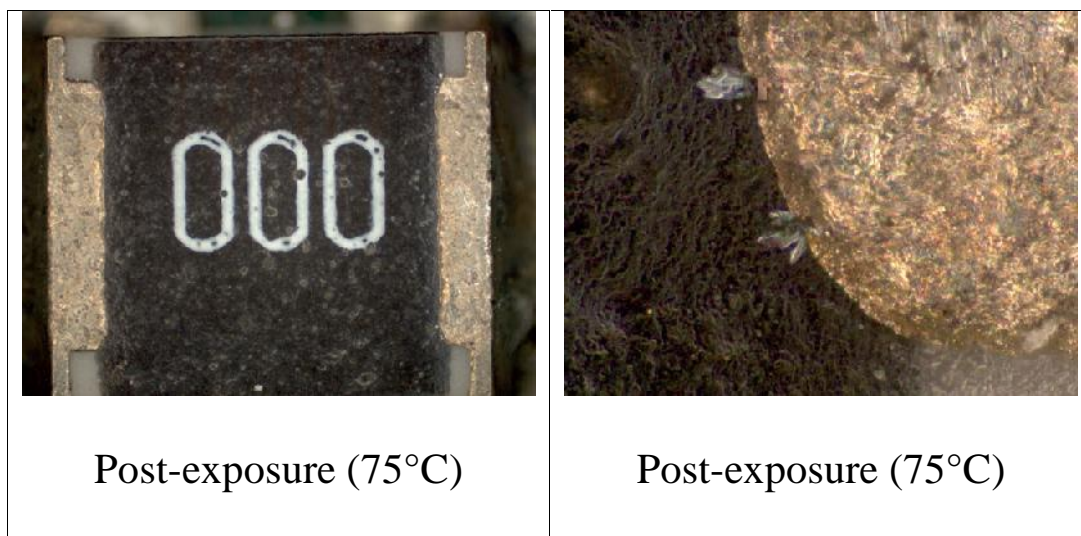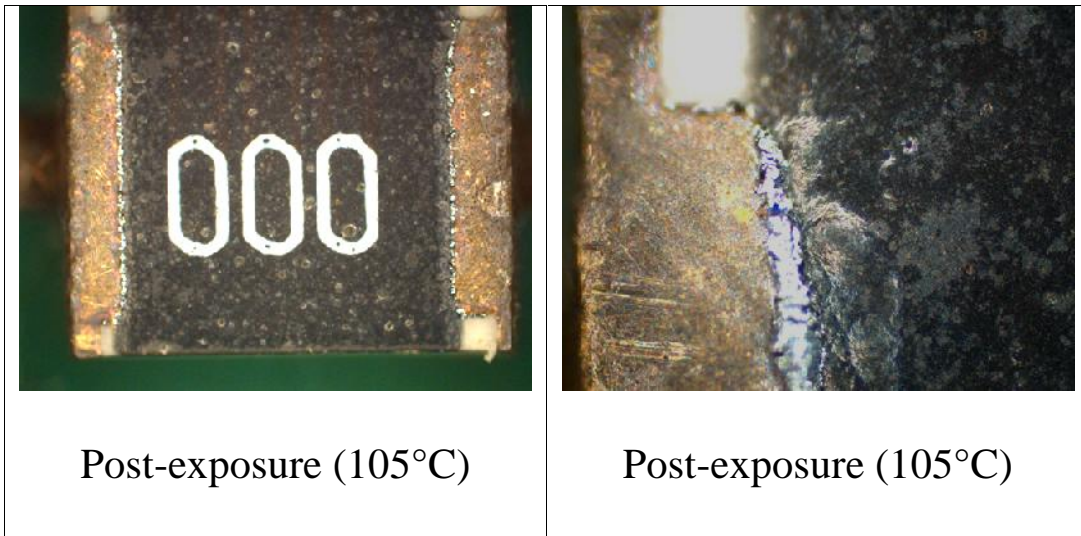
**Figure 31. Chip resistors in high temperature FOS tests**

High temperature FOS testing (above 75°C) is useful for corrosion testing of OSP finished boards and chip resistors. Increasing FOS test temperatures above 75° did not change the appearance of corrosion products on ENEPIG or ImAg finished boards.

# Appendix 4: ANalysis Of Variance

| P values | | 50C | | | | 75C | | 85C | | | | 95C | | 105C | | |
|---|---|---|---|---|---|---|---|---|---|---|---|---|---|---|---|---|
| | | 1 day | 5 day | 10 day | 15 day | 1 day | 10 day | 1 day | 5 day | 10 day | 15 day | 1 day | 10 day | 1 day | 5 day | 10 day |
| 50C | 1 day | ■ | 3.28E-01 | 2.01E-01 | 8.28E-02 | 1.04E-01 | 9.37E-04 | 4.17E-04 | 6.42E-03 | 5.04E-06 | 8.49E-06 | 3.37E-03 | 9.08E-04 | 1.05E-04 | 5.18E-06 | 2.90E-04 |
| | 5 day | 3.28E-01 | ■ | 3.40E-01 | 1.36E-01 | 2.04E-01 | 9.82E-04 | 9.21E-04 | 7.12E-03 | 5.46E-06 | 8.54E-06 | 5.60E-03 | 9.16E-04 | 2.17E-04 | 5.61E-06 | 2.92E-04 |
| | 10 day | 2.01E-01 | 3.40E-01 | ■ | 5.53E-01 | 8.90E-01 | 1.28E-03 | 6.61E-01 | 1.06E-02 | 9.74E-06 | 8.79E-06 | 4.87E-02 | 9.43E-04 | 4.51E-03 | 9.92E-06 | 2.99E-04 |
| | 15 day | 8.28E-02 | 1.36E-01 | 5.53E-01 | ■ | 6.02E-01 | 1.41E-03 | 6.82E-01 | 1.36E-02 | 1.12E-05 | 8.92E-06 | 1.19E-01 | 9.62E-04 | 9.78E-04 | 1.14E-05 | 3.04E-04 |
| 75C | 1 day | 1.04E-01 | 2.04E-01 | 8.90E-01 | 6.02E-01 | ■ | 1.21E-03 | 7.45E-01 | 1.05E-02 | 8.27E-06 | 8.76E-06 | 4.08E-02 | 9.45E-04 | 2.78E-03 | 8.44E-06 | 3.00E-04 |
| | 10 day | 9.37E-04 | 9.82E-04 | 1.28E-03 | 1.41E-03 | 1.21E-03 | ■ | 1.07E-03 | 1.45E-03 | 3.84E-02 | 3.24E-04 | 1.56E-03 | 1.41E-02 | 1.78E-03 | 3.74E-02 | 5.23E-03 |
| 85C | 1 day | 4.17E-04 | 9.21E-04 | 6.61E-01 | 6.82E-01 | 7.45E-01 | 1.07E-03 | ■ | 1.01E-02 | 5.74E-06 | 8.70E-06 | 1.85E-02 | 9.48E-04 | 2.90E-04 | 5.90E-06 | 3.00E-04 |
| | 5 day | 6.42E-03 | 7.12E-03 | 1.06E-02 | 1.36E-02 | 1.05E-02 | 1.45E-03 | 1.01E-02 | ■ | 3.49E-04 | 1.23E-05 | 2.50E-02 | 1.37E-02 | 5.45E-02 | 3.46E-04 | 4.13E-04 |
| | 10 day | 5.04E-06 | 5.46E-06 | 9.74E-06 | 1.12E-05 | 8.27E-06 | 3.84E-02 | 5.74E-06 | 3.49E-04 | ■ | 1.96E-05 | 1.06E-05 | 3.86E-03 | 1.04E-05 | 9.43E-01 | 9.28E-04 |
| | 15 day | 8.49E-06 | 8.54E-06 | 8.79E-06 | 8.92E-06 | 8.76E-06 | 3.24E-04 | 8.70E-06 | 1.23E-05 | 1.96E-05 | ■ | 9.15E-06 | 3.96E-03 | 9.41E-06 | 1.96E-05 | 1.16E-02 |
| 95C | 1 day | 3.37E-03 | 5.60E-03 | 4.87E-02 | 1.19E-01 | 4.08E-02 | 1.56E-03 | 1.85E-02 | 2.50E-02 | 1.06E-05 | 9.15E-06 | ■ | 1.02E-03 | 4.14E-02 | 1.08E-05 | 3.18E-04 |
| | 10 day | 9.08E-04 | 9.16E-04 | 9.43E-04 | 9.62E-04 | 9.45E-04 | 1.41E-02 | 9.48E-04 | 1.37E-02 | 3.86E-03 | 3.96E-03 | 1.02E-03 | ■ | 1.08E-03 | 3.88E-03 | 2.01E-01 |
| 105C | 1 day | 1.05E-04 | 2.17E-04 | 4.51E-03 | 9.78E-04 | 2.78E-03 | 1.78E-03 | 2.90E-04 | 5.45E-02 | 1.04E-05 | 9.41E-06 | 4.14E-02 | 1.08E-03 | ■ | 1.07E-05 | 3.34E-04 |
| | 5 day | 5.18E-06 | 5.61E-06 | 9.92E-06 | 1.14E-05 | 8.44E-06 | 3.74E-02 | 5.90E-06 | 3.46E-04 | 9.43E-01 | 1.96E-05 | 1.08E-05 | 3.88E-03 | 1.07E-05 | ■ | 9.33E-04 |
| | 10 day | 2.90E-04 | 2.92E-04 | 2.99E-04 | 3.04E-04 | 3.00E-04 | 5.23E-03 | 3.00E-04 | 4.13E-04 | 9.28E-04 | 1.16E-02 | 3.18E-04 | 2.01E-01 | 3.34E-04 | 9.33E-04 | ■ |

P-values for a 2-sided F-Test. Highlighted values are P>.1, meaning that there is less that a 90% chance that the two test groups could come from different populations given their variance. Analysis in chapter 4 examines specific findings from the ANOA data.

**Introduction**

The Flowers of Sulfur (FOS) test can be used to carry out lifetime testing for electronic components that are subjected to sulfur-driven corrosion in their field environment. This document outlines the apparatus and method for selecting test parameters based on achieving a desired target.

The major assumptions of this test is that sulfur-driven corrosion is the main component of the corrosion process observed on fielded samples. Energy Dispersive X-ray Spectroscopy (EDS) can be performed on fielded samples in order to verify that the corrosion products are sulfur-based. In cases where there are other contaminants that appear to affect the corrosion of the electronic part, this test may not be representative of the field environment, but instead may serve as an estimate for what would happen if the corrosion film seen in the field were only caused by sulfur-driven corrosion.

**Test Setup**

The test setup described below was selected to be easily reproducible in order to have consistent results. Figure 32 shows a schematic of the test setup. A 10-liter glass desiccator is used as the test vessel. Sublimed sulfur (from Fisher Scientific) is placed into a 15 cm diameter petri dish that is placed on the bottom of the desiccator dish. A saturated potassium nitrate (>99%, Fisher Scientific) salt solution (200 g $KNO_3$ in 200 mL $H_2O$) is poured into a 15 cm diameter petri dish that is placed on the bottom

of the desiccator. Samples are hung from a stand that is placed in the center of the test vessel. This stand and the sample hangers should be made of a non-reactive material, such as glass. Samples should be kept 7.5 cm from the sulfur source, 2.5 cm from the side walls of the chamber, and 1 cm from other samples. The test vessel is placed into an over that can achieve the target temperature for the target duration.
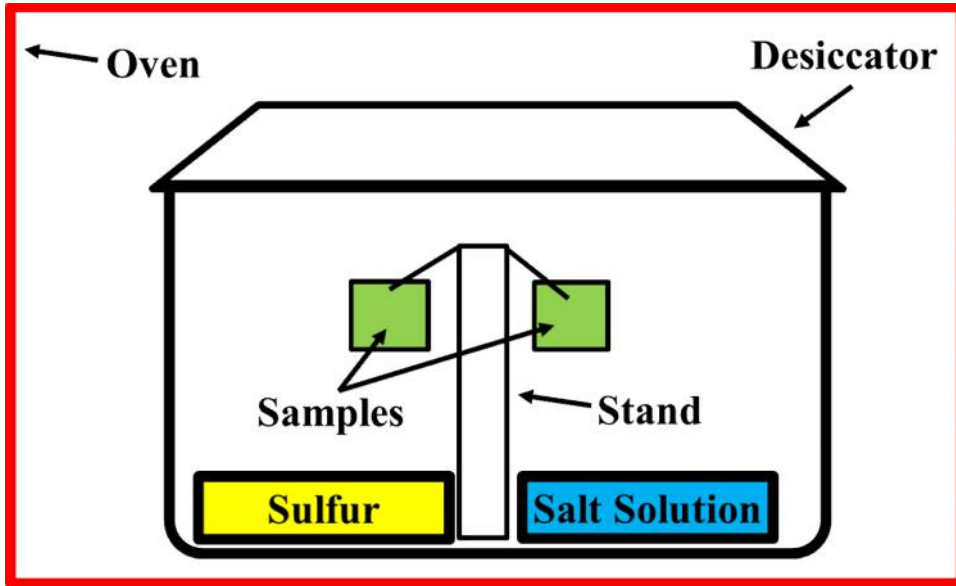


**Figure 32. Flowers of Sulfur Test Schematic**

**Selecting Test Conditions**

The test time and temperature for the FOS test is selected based on expectations for the expected field condition. The amount of corrosion expected in a particular field condition can be monitored using copper witness coupons in the environment and measuring the corrosion film thickness. Using field data, an estimate of the corrosion film thickness ( ) can be determined. Either the test temperature (T in °C) or the test duration (t in hours) can be fixed, and the other can be determined using Equation 4.

$$= 2.3 * e^{.0706T} * e^{.0132t}$$

**Equation 4. Corrosion thickness for FOS temperature and duration**

**Application Notes**

Test conditions should not be used if they fit into any of the following criteria as the method described in this document has either not been tested or has been found insufficient as an estimate. Test conditions should be rejected if they have (1) test temperatures outside of a 50C to 105C range, (2) test durations less than one day or longer than 15 days, or (3) a 1 day Test duration with a test temperature below 90°C

# Bibliography

1. R. Revie. "Corrosion and Corrosion Control", John Wiley and Sons, Inc., Hokoken, New Jersey. (2008)

2. P. Schweitzer. "What every engineer should know about Corrosion", Marcel Decker, Inc., Chester, New Jersey. (1987)

3. J. West. "Basic Corrosion and Oxidation", Ellis Horwood Limited. New York, New York. (1986)

4. W. Kirk and H. Lawson. "Atmospheric Corrosion", ASTM. Philadelphia, Pennsylvania. (1995)

5. American Society for Testing and Materials (ASTM). "Corrosion in Natural Environments", ASTM, Philadelphia, Pennsylvania. (1973)

6. Rice et al. "Atmospheric Corrosion of Copper and Silver" Journal of the Electrochemical Society 128.2 (1981)

7. W. Abbott. "The corrosion of copper and porous gold in flowing mixed gas environments". IEEE Transactions on components, hybrids, and manufacturing technology 13.1 (1990)

8. C. Leygraf and T. Graedel. "Atmospheric Corrosion", Wiley-Interscience. New York, New York. (2000)

9. ASTM Standard B810 - 01a, 2011, "Standard Test Method for Calibration of Atmospheric Corrosion Test Chambers by Change in Mass of Copper

Coupons," ASTM International, DOI: 10.1520/B0810-01AR11, www.astm.org (2011)

10. P. Mazurkiewicz, "Accelerated corrosion of PCBs due to high levels of reduced sulfur gasses in industrial environments," Proceedings of the 32nd International Symposium for Testing and Failure Analysis, Austin, TX (2006)

11. G. Dieter and L. Schmidt. "Engineering Design", Mc-Graw Hill Higher Education. Boston, MA. (2009)

12. ASTM Standard B765 -03, 2013, "Standard Guide for Election of Porosity and Gross Defect Tests for Electrodeposits and Related Metallic Coatings" ASTM International, DOI: 10.1520/B0765, www.astm.org (2013)

13. W. Abbott. "The development and performance characteristics of flowing mixed gas test environments". IEEE Transactions on Components, Hybrids, and Manufacturing Technology (1988)

14. Electronic Industries Association, EIA Standard TP-65A (1998)

15. W. Wang, A. Choubey, M. Azarian, and M. Pecht, "An assessment of immersion silver surface finish for lead-free electronics," Journal of Electronic Materials, Vol. 38, No. 6, pp. 815-827. (2009)

16. Laskowski et al. "Indoor Corrosion of Metals" Journal of the Electrochemical Society 127.4 (1980)

17. L. Greenspan. "Humidity Fixed Points of Binary Saturated Aqueous Solutions" Journal of Research of the National Bureau of Standards 81A.1 (1977)

18. E.W. Washburn, International Critical Tables of Numerical Data, Physics, Chemistry and Technology. [1st Electronic Edition] (1926 – 1930)

19. R. Veale, "Reliability of PCB Alternate Surface Finishes In A Harsh Industrial Environment," SMTA International. (2005)

20. C. Xu et al., "Corrosion resistance of PWB final finishes," Alcatel-Lucent, APEX 2007, Los Angeles, CA. (2007)

21. S. Zhang, M. Osterman, A. Shrivastava, R. Kang, M. Pecht, "The Influence of H2S exposure on immersion silver finished PCBs under mixed flow gas Testing", IEEE Transactions on Device and Materials Reliability, Vol. 10, No. 1. (2010)

22. ASTM Standard B809-95, 2013, " Standard Test Method for Porosity in Metallic Coatings by Humid Sulfur Vapor ("Flowers-of-Sulfur")," ASTM International, DOI: 10.1520/B0809, www.astm.org (2013)

23. R. Schueller, "Creep Corrosion on Lead-free Printed Circuit Boards in High Sulfur Environments", SMTA International Conference, Orlando, Fl, pp. 643-654. (2007)

24. Y. Zhou and M. Pecht. "Investigation on Mechanism of Creep Corrosion of Immersion Silver Finished Printed Circuit Board by Clay Tests", 55th Annual IEEE Holm Conference, Vancouver, British Columbia, Canada, pp. 321-330. (2009)

25. ANSI/ISA 71.04-1985, Environmental Conditions for Process Measurement and Control Systems: Airborne Contaminants. The Research Triangle Park, NC: Instrumentation, Systems and Automation Society. (2985)

26. ASHRAE. "2011 Gaseous and Particulate Contamination Guidelines of Data Centers", American Society of Heating, Refrigerating and Air-Conditioning Engineers white paper. (2011)

27. B. Hindin and J. Fernandez. "Testing of Conformal Coatings Using the Flowers-of-Sulfur Test". Tri-Service Corrosion Conference. (2003)

28. B. Hindin and M. Pledger. "Silver Sulfidation Kinetics in Flowers of Sulfur Environment". Proceedings of SMTAI (2014)

29. T. Tofil et al. "Harsh Environmental Impact on Resistor Reliability", SMTAI. (2010)

30. S. Axtell. "Failure of Thick-Film Chip Resistors in Sulfur-Containing Environments" Proc. of CARTS 2002. (2002)

31. M. Reid, M. Collins, E. Dalton, J. Punch, and D. Tanner. "Testing method for measuring corrosion resistance of surface mount chip resistors". Microelectronics Reliability (2012)

32. H. Fu, P. Singh, L. Campbell, J. Zhang, W. Ables, D. Lee, J. Lee, J. Li, S. Zhang, and S. Lee. "Testing Printed Circuit Boards for Creep Corrosion in Flowers of Sulfur Chamber". IPC APEX EXPO 2014 (2014)

33. H. Fu, P. Singh, and J. Zhang, "Creep corrosion test in flowers of sulfur chamber". 2014 International Conference on Electronics Packaging (ICEP). (2014)

34. A. Khanna. "High Temperature Oxidation and Corrosion", ASM International. Materials Park, OH. (2002)

35. B. Meyer. "Elemental Sulfur." Chemical Reviews 176.3. (1976)